

PSFC/RR-03-6

**In-Situ Conductance and Flow Measurements Through Alcator C-Mod Divertor
Structures With and Without Plasma Present**

B. LaBombard and C. Boswell

1/27/2003

Plasma Science and Fusion Center
Massachusetts Institute of Technology
Cambridge, MA 02139 USA

This work was supported by the U.S. Department of Energy, Cooperative Grant No. DE-FC02-99ER54512. Reproduction, translation, publication, use and disposal, in whole or in part, by or for the United States government is permitted.

In-Situ Gas Conductance and Flow Measurements Through Alcator C-Mod Divertor Structures With and Without Plasma Present

B. LaBombard and C. Boswell 1/27/03

A specialized arrangement of gas-puff capillaries and in-situ pressure gauges has been installed in Alcator C-Mod to allow gas conductances and flows around divertor structures to be measured with or without plasma present in the chamber. Results are presented from a series of dedicated experiments performed during the 1020725 run day (MP#313, “Instrumented Divertor Leakage Experiments”). Gas conductances and flows are compiled in this report with the aim of providing good benchmark points for numerical simulations of gas flow and “plasma plugging” physics in Alcator C-Mod. A strong plasma plugging effect is found at locations where the divertor structure is opened for diagnostics access (the so-called “open-port” locations), as evidenced by a factor of ~ 4 reduction in the local gas conductance with plasma present. The effect is most dramatic for locations in the upper chamber region where there is no neutral baffle structure; a factor of ~ 5 reduction in the local gas conductance is found there. Gas conductance through an open divertor flap is measured to be a factor of ~ 3 lower than that which has been commonly assumed using the area of the open flap. The conductance through the flap is found to be similar with or without plasma present, indicating that there is no “plasma plugging” effect occurring at this location. The gas flow rate through a flap that is adjacent to an “open-port” location is found to be a factor of 2 lower than at a location distant from open ports. The latter result suggests that significant toroidal variations in the pressures exist under the lower divertor modules.

I. Introduction

Modeling of neutral transport in the divertor of Alcator C-Mod with state-of-the-art numerical codes has lead to a puzzle: the predicted pressures behind the outer divertor module are a factor of 2 to 10 times lower than that which is observed in experiment [1,2]. Given the extensive plasma/neutral/wall physics that is included in these models, there is only a limited number of possible explanations for the discrepancy, including: (1) the pressure measurements in the divertor are in error, (2) the neutral conductances through leakage pathways are numerically incorrect, either because of geometrical complications or because there are plasma-neutral interaction effects that are unaccounted for (the so-called “plasma plugging” explanation), (3) neutral sources (via surface- and

volume- recombination) in the divertor region are being underestimated (and inaccurately measured via optical diagnostics), or (4) some combination of the above.

In addition, there is the observation that neutral pressures in the upper divertor during upper x-point discharges are comparable to neutral pressures in an open section of the lower divertor during lower x-point discharges [3]. This suggested that perhaps some combination of fast radial transport to the walls (main-chamber recycling) and a “plasma plugging” phenomenon may be setting the divertor neutral pressures rather than the details of the vacuum conductances through the mechanical structures.

In order to help identify the effect(s) responsible for the mismatch between modeling and experiment, a series of hardware modifications and experiments were recently proposed for C-Mod [4] which would allow the gas conductance and flow through various mechanical structures, including the divertor bypass flappers, to be directly measured. During the vacuum break and maintenance period of September 2001 to May 2002, a specialized set of hardware was installed just for this purpose. The hardware included a set of pressure gauges [both in-vessel gauges (Penning) and ex-vessel gauges (ionization and Baratron type)] and a set of gas capillary tubes, specifically located near pressure measurement points. The idea was to run a reference discharge with no capillary puffs and record the pressures. Then repeat discharges with known capillary gas throughput at a variety of locations and measure the neutral pressures again (focussing on their change). From this, the effective gas conductance would be quantified (i.e., relationship between gas throughput and pressure difference) to volumes away from the points of the gas injection. The conductance would be “effective” in the sense that it includes effects due to the presence of the plasma. By puffing gas and recording pressure changes without plasma, the vacuum conductance would also be measured. Conductances measured with and without plasma could then be used to constrain numerical modeling -- the same “experiment” could be done in numerical simulations; we would then know when the code has a good model (or not) for the effective gas conductances through the divertor and other leaks.

New capillaries were also installed just above the C and D-divertor flaps, locations that are in the view of the divertor-viewing camera, DIV2. The idea was to puff a known flow rate of D_2 molecules through these capillaries and record the resultant change in D_α emission above the flaps. This would serve to calibrate the camera’s D_α brightness in terms of a local gas injection rate. Then the change in D_α brightness recorded when the flap was opened could be used as an absolute measure of the gas flow through the flap.

This report describes a set of gas conductance and flow measurements that were made during the 1020725 run which was dedicated to such experiments (Miniproposal #313, “Instrumented Divertor Leakage Experiments”). Section II describes the pressure measurement locations, divertor geometry, capillary gas puff locations, and D_{α} camera view. Section III describes the results from a series of experiments, each involving one or two discharges that were designed to allow the gas conductance and/or flow at a variety of locations in the vacuum vessel to be deduced. Gas conductance and flow measurements are tabulated and summarized in section IV.

II. Experimental Arrangement

Figures 1 and 2 show plan-views of the floor tiles, divertor tiles, and vertical ports in Alcator C-Mod (Fig.1 - floor level, Fig.2 - level just above outer divertor). Figure 3 shows a similar view of the ceiling tiles (looking up from below). Note that the DIV2 camera view includes regions above the C- and D-divertor flaps (Fig.2). Cross-sectional views of the torus at “B”, “BC”, and “E” are shown in Figs. 4, 5, and 6, respectively. These locations are of particular interest, having pressure gauges and gas-puff capillaries. Note that in Figs. 4 and 6 the vertical ports are artificially shortened so as to fit on the page. (For reference, the diameter of the flanges on the 4-way crosses are 16 inches. The region between the double horizontal lines on Figs. 4 and 6 should actually be 41 inches, not 1 inch as shown.) The “CB DivU” Penning gauge was not operating during this run day (had a shorted cable), so no experiments were performed with the “B-C Top” capillary.

A few discharges with a short-duration plasma current waveform but a long-duration toroidal field waveform (TF) were first run (shots 2,3,4). After plasma termination the neutral pressure in the chamber rapidly equilibrates. Therefore, after plasma termination but while the toroidal field is still at full strength the pressure readings on the “CB_DivL” Penning gauge and the capacitance manometers were compared. These readings verified that the CB_DivL Penning gauge calibration was accurate. The CB_DivL Penning gauge signal sometimes exhibited what appear to be “mode-jumps”; the pressure reading jumps up or down by 10% or so. This is a typical behavior for Penning gauges. So we need to be careful in interpreting the pressure readings. Nevertheless, in comparing the Penning gauge response for a number of

identical discharges (for example see Figs. 16 and 19 below), one can see that the gas conductances deduced from the Penning gauge measurements are reliable.

All other gauges that were used for these experiments [G-Side MKS (0 to 0.1 torr range), B-Bottom MKS (0 to 1 torr range), E-Bottom MKS (0 to 1 torr range), and E-Top MKS (0 to 0.1 torr range)] are capacitance manometer gauges. These gauges are independent of gas species and are normally very accurate (< ~5% level) in the few mtorr range. A cross-comparison of pressure readings after at discharge verifies their relative accuracy. (For example, see Figs. 10, 14, 17 and 21.)

The DIV2 camera was filtered for D_{α} light and had a clear view of regions just above the C- and D-divertor flaps. Images from the DIV2 camera are stored at a standard video field rate of 60 Hz. Figures 7 and 8 show images taken before and during gas puffs through the capillaries above the C and D divertor flaps, respectively. Brightness signals corresponding to regions above the C- and D-divertor flaps are generated for each video field by summing signals from pixels which view the relevant regions (regions are defined by the rectangular boxes shown in Figs. 7 and 8).

All discharges were produced with the pumping-stack gate valves closed, i.e., there was no particle exhaust from the torus during the discharge and for a period of time of about a one minute after the discharge ended. This allowed a direct measurement of the gas flow rate through the capillary that was used during any given shot. Figure 9 illustrates the method, using data from shot #1020725011 as an example. The B-Bottom capillary was triggered twice with identical time durations (trigger#1: 0.2 s, duration 1.8 s, trigger#2: 2.7 s, duration 1.8 s). Note that owing to the sequential operation of the solenoid and pneumatic valves that admit gas into each capillary, there is a slight delay between the trigger times and the time that gas first enters the vacuum chamber. Since the gas plenum feeding the capillary has a large volume, the drive pressures are virtually identical during both puffs. Therefore, the gas flow rate measured during the second puff (as inferred from the increase in pressure of a vessel with known volume) can be taken as the same as for the first puff. This technique was employed for every discharge during this run day. In the analysis that follows, the gas flow rate waveform that is shown for a given capillary is simply taken as the flow rate for the second puff, but displaced in time to correspond to the time of the first puff.

III. Gas Conductance and Flow Experiments

A. Conductance at location “B-Bottom”

The vacuum conductance for gas puffed through the B-Bottom capillary was computed from shot 1020725011, as shown in Fig. 10. The data shown here were taken

after the end of the discharge while all gate valves remained closed. Gas puffed through the B-Bottom capillary arrives in a “closed port” section of the divertor (see Fig. 4). The B-Bottom MKS gauge responds to the gas flow with a step-change in pressure. The gas flow (computed to be about 15 torr-liters/s) results in a pressure difference between B-Bottom and G-Side MKS gauges of about 12 mtorr which yields a conductance of 1200 liters/s.

In order to compute the conductance at the same location but with plasma present, it is necessary to compare B-Bottom MKS pressure gauge readings between two shots: Both shots must be identical except that one must have gas puffed through the B-Bottom capillary and the other must not. Figure 11 shows data taken during a “background” discharge (shot #1020725009), i.e., one where gas was puffed through a capillary mounted at the outer midplane on the A-B split limiter. (The same capillary as that used for the gas-puff turbulence imaging system.)

Figure 12 shows data taken during a very similar discharge (shot #1020725011), except that the gas was puffed through the B-Bottom capillary. Note the increase in pressure on the B-Bottom MKS gauge.

Figure 13 shows a computation of the “effective conductance” (i.e., a conductance in the presence of plasma) for gas introduced through the B-Bottom capillary, using data from shots #1020725011 and #1020725009. The computation yields an effective conductance of 700 liters/s, significantly reduced relative to the vacuum conductance.

B. Conductance at location “E-Bottom”

The vacuum conductance for gas puffed through the E-Bottom capillary was computed from shot 1020725012, as shown in Fig. 14. The analysis is similar to that of Fig. 10, yielding a vacuum conductance of 4500 liters/s.

Figure 15 shows data taken during the plasma phase of shot #1020725012, which was identical to shot #1020725009, except that the gas was puffed through the E-Bottom capillary. Note the increase in pressures on the E-Bottom MKS gauge.

Figure 16 shows a computation of the effective conductance for gas introduced through the E-Bottom capillary, using data from shots #1020725012 and #1020725009. The computation yields an effective conductance of 1200 liters/s, a dramatic reduction relative to the vacuum conductance.

C. Conductance at location “E-Top” in SNL discharge

Experiments described in this and the following sections focussed on conductances at the “E-Top” location. As one might expect, the effective conductance was found to be influenced by whether the discharge was run in a lower or upper single-

null configuration (SNL or SNU). Here we look at the response to a standard lower single null discharge similar to the background shot, #1020725009.

The vacuum conductance for gas puffed through the E-Top capillary was computed from shot 1020725013, as shown in Fig. 17. The analysis is similar to that of Fig. 10, yielding a vacuum conductance of 5000 liters/s.

Figure 18 shows data taken during the plasma phase of shot #1020725013, which was identical to shot #1020725009, except that the gas was puffed through the E-Top capillary. Note the increase in pressures on the E-Top MKS gauge.

Figure 19 shows a computation of the effective conductance for gas introduced through the E-Top capillary, using data from shots #1020725013 and #1020725009. The computation yields an effective conductance of 2200 liters/s, which is a remarkable reduction relative to the vacuum conductance, especially considering that this was a lower single-null discharge.

D. Conductance at location “E-Top” in SNU discharge

Now we look at the conductances at E-Top in response to an upper single null discharge. First we need a new SNU “background” shot. This shot is #10207025023. Figure 20 shows the time-traces for this discharge. Gas was puffed through a capillary mounted at the outer midplane on the A-B split limiter so as to produce discharge time-traces that are similar to one with gas puffed through the E-Top capillary.

The vacuum conductance for gas puffed through the E-Top capillary was computed again, this time from shot #1020725024 (shown in Fig. 21). The analysis is identical to that of Fig. 17, yielding a vacuum conductance of 5200 liters/s. This result shows that the conductance can be reproducibly computed to within about 5%.

Figure 22 shows data taken during the plasma phase of shot #1020725024, which was nearly identical to shot #1020725023, except that the gas was puffed through the E-Top capillary. Note the increase in pressures on the E-Top MKS gauge.

Figure 23 shows a computation of the effective conductance for gas introduced through the E-Top capillary, using data from shots #1020725024 and #1020725023. The computation yields an effective conductance of 1100 liters/s during the times when the discharges are well matched. Thus, the effect of a SNU X-point is to further reduce the effective vacuum conductance at the E-Top location.

E. Vacuum conductance at “B-C Bottom” and through the C-Divertor Flap

In order to measure the vacuum conductance for gas puffed through the B-C Bottom capillary, the CB_DivL Penning gauge must be used. But the Penning gauge requires magnetic field to operate. Also, the Penning gauge does not turn on very easily; it usually starts up only during the plasma breakdown phase. So to perform this measurement, a short plasma discharge was run with the toroidal magnetic field programmed to stay on longer. Figure 24 shows the resultant time traces over the time range of 0.9 to 2.6 seconds. The C-divertor flap was opened/closed during this time while gas was puffed through the BC-Bottom capillary. The modulation in the CB_DivL Penning gauge signal over the time span of 1.12 to 1.8 seconds looks clean and reliable.

Figure 25 shows a computation of the vacuum conductance for gas puffed through the BC-Bottom capillary while the C-divertor flap was opened and closed. When the flap is closed, the vacuum conductance is 1400 liters/s. However, when the flap is opened, the conductance increases to 2100 liters/s. This indicates that an open flap has a vacuum conductance of 700 liters/s. This number is a factor of 3 below that which has been commonly assumed for the flap conductance (2300 liters/s), a simple estimate based on using the exposed area of an open flap [5].

F. Gas conductance and flow through divertor flaps via D_{α} measurements

1. Experimental setup

The DIV2 camera view in conjunction with the capillaries located above the C and D-divertor flaps were used to determine the gas flow rate through the respective divertor flaps. In addition, from the pressure measured under the C-divertor flap, the effective conductance through that flap was estimated. Shots 1020725026 and 1020725030 were the best shots for these experiments. The core plasma conditions of these shots evolved identically in time but each had a short, strong puff of gas through the B-C Flap capillary (1020725026) and the C-D Flap capillary (1020725030), followed by a time period where the respective divertor flaps were opened/closed for three cycles. By trial-and-error optimization performed during previous shots, the capillary gas puffs were adjusted so that the step increase in D_{α} seen by the DIV2 camera was of similar magnitude to the step increase seen when the divertor flap was opened. Since the capillary gas puff flow rate could be absolutely calibrated for any shot, the gas flow through the flap could be determined by comparing the relative change in D_{α} light levels.

During the time of the capillary gas puff in these discharges, the core plasma density increased sharply. This caused the D_{α} light levels to also promptly increase everywhere. Thus, rather than just looking at the local change in D_{α} light levels near the

capillary/flap for a given shot, it is important to compare the change in local D_{α} light levels relative to a background shot. Gas flow through the C-divertor flap was therefore deduced from shot 1020725026 using 1020725030 as the background while flow through the D-divertor flap was deduced using 1020725030 compared to 1020725026 as background.

Figures 26 and 27 show the usual set of time-traces for shots 1020725026 and 1020725030. Figure 28 shows the trigger-programming of two identical gas puffs on shot 1020725026 and the resultant change in gas inventory. In the analysis that follows, the flow rate signal for the first gas puff is taken to be identical to the flow rate signal for the second gas puff, computed from the change in gas inventory (with appropriate displacement in time axis).

2. Conductance and flow rate through C-divertor flap

Figure 29 shows signals used to compute of the gas flow rate and effective gas conductance through the C-divertor flap. The good match between NL04 signals in the top panel of Fig. 29 shows that shot #1020725030 provides a background for comparing D_{α} light levels over the C-divertor flap. On shot #1020725030, the D_{α} light level detected by the DIV2 camera over a region just above the C-divertor flap (see camera view in Fig.7) corresponds to the case of no local gas puff and no C-divertor flap movement. Therefore, any increase in D_{α} light above this level seen on shot #1020725026 can be ascribed to an increase in local gas/plasma interaction, caused either by gas flow through the capillary located above the C-divertor flap or by gas flow through the opening of the C-divertor flap.

A calibration factor (BC_CAL) that converts the sum of D_{α} light signals from the DIV2 camera (DIV2_BC_SIG) to local gas injection rate (DIV2_BC) can be defined,

$$\text{DIV2_BC} = \text{BC_CAL} * \text{DIV2_BC_SIG} . \quad (1)$$

The calibration factor can be determined by requiring that DIV2_BC obtained from shot#1020725026 agree with the same signal obtained from shot#1020725030 (DIV2_BC_30), accounting for the gas puffed through the B-C Flap capillary on shot#1020725026 and looking only during times when the C-divertor flap was closed,

$$\text{DIV2_BC} = \text{DIV2_BC_30} + \text{BC_FLAP_CAP}, \quad (2)$$

requiring that

$$BC_CAL = BC_FLAP_CAP / (DIV2_BC_SIG - DIV2_BC_SIG_30) . \quad (3)$$

The second panel in Fig. 29 shows gas flow signals constructed using this procedure. The summed signals, DIV2_BC_30 + BC_FLAP_CAP (red), overlay with the signal DIV2_BC (blue) during the times when the C-divertor flap is closed, indicating that a good estimate for BC_CAL has been obtained. The gas flow through the open flap can be read directly from the difference between the red and blue traces - approximately 25 torr-liter/s in this case.

The effective conductance of the open flap (last panel of Fig. 29) is computed from the gas flow through the flap divided by the pressure under the C-divertor flap minus the midplane pressure gauge reading (G-Side MKS). Note that there appear to be some “mode-jumps” in the CB_DivL Penning gauge, adding a bit of uncertainty to the pressure under the C-divertor flap. Nevertheless, effective conductances of about 800 liters/s are obtained. These are essentially identical to the vacuum conductances derived in section III.E. Thus, there appears to be no plasma plugging effect for gas flowing through the flap.

3. Flow rate through D-divertor Flap

Figure 30 shows signals that are used to compute of the gas flow rate and effective gas conductance through D-divertor flap. The analysis is identical to that outlined for the C-divertor flap above, with the exception that there is no pressure gauge under the D-divertor flap.

The summed signals, DIV2_CD_26+CD_FLAP_CAP (red), overlay with the signal DIV2_CD (blue) during the times when the D-divertor flap is closed, indicating that a good estimate for CD_CAL has been obtained. The gas flow through the open flap can be read directly from the difference between the red and blue traces - approximately 10 torr-liter/s in this case. The flow rate is a factor of 2 below that seen through the C-divertor flap. This may be caused by a lower pressure under the D-divertor flap; the D-divertor module is next to an “open-port” (D-port, as shown in Fig.2), which may lead to lower pressures there.

IV. Summary and Conclusions

Measurements of gas conductance and flow from discharges during the 1020725 run day are summarized in Table I.

Table I - Summary of Gas Conductance and Flow Measurements

Location	Conductance (liters/s)		Corresponding shot numbers	
	Vacuum	with Plasma	Vacuum	with Plasma
BC divertor:				
Flap Open	2100		1020725005	
Flap Closed	1400		1020725005	
Open C Flap	700	800	1020725005	1020725026 (_030 baseline)
B-Bottom	1200	700	1020725011	1020725011 (_009 baseline)
E-Bottom	4500	1200	1020725012	1020725012 (_009 baseline)
E-Top:SNL	5000	2200	1020725013	1020725013 (_009 baseline)
E-Top:SNU	5200	1100	1020725024	1020725024 (_023 baseline)

Location	Leakage (torr-l/s)	Corresponding shot numbers
Open C Flap	25	from Div2: 10207250026 (_030 baseline)
Open D Flap	10	from Div2: 10207250030 (_026 baseline)

As a result of these experiments, the following conclusions about gas flow and leakage through the Alcator C-Mod divertor structures can be drawn:

- (1) Although the gas flow rate through the divertor flap is found to be a factor of 3 lower than that computed from the area of an open flap (700 liters/s versus 2300 liter/s), it is unchanged by the presence of plasma (at least in the discharges studied here), i. e., there is no “plasma plugging” effect at this location.
- (2) A moderate or strong plasma plugging effect does occur at all other locations studied. The strongest effect occurs at the E-Top location for SNU discharges - a factor of ~5 reduction in the effective gas conductance.
- (3) The E-Top and E-Bottom locations behave in an almost a symmetric way: Strong plasma plugging occurs for these locations when the active divertor is near to that location. This result is consistent with the observation of E-Top pressures in SNU discharges that are comparable to E-Bottom pressures in SNL discharges.
- (4) Even in a SNL discharge, strong plasma plugging is observed in the upper chamber; the presence of plasma results in a factor of ~2.5 reduction in the gas conductance at the E-Top location.

- (5) The gas leakage rate through the C- and D-divertor flap was found to be different by a factor of 2 in the same discharge. This indicates that a substantial toroidal variation in the gas flow through the flaps is likely, probably associated with the proximity of the flap to “open” versus “closed-port” locations.

These conclusions are encouraging for the performance of an upper cryopump: A simple baffle structure could be constructed to cover the region in the upper divertor where plasma plugging is not likely to be active - the location symmetrical to the lower divertor flap location. With a baffle structure that closes this region to neutral flux (yet does not protrude into the high heat flux plasma region), the pressures in the upper chamber during near-balanced double-null discharges (with the lower X-point remaining dominant to send the heat flux towards lower divertor) might be increased to a level comparable to present B-Bottom pressures.

Conclusion (5) suggests that a significant increase in the pressures under the lower divertor could be obtained by reducing the toroidal leakage pathways into the “open ports”.

References

- [1] D. Stotler, *et al.*, “Understanding of Neutral Gas Transport in the Alcator C-Mod Tokamak Divertor”, presented at the 13th APS Topical Conference on Atomic Processes in Plasmas, Gatlinburg, Tennessee, April, 2002.
- [2] S. Lisgo, *et al.*, “EIRENE Neutral Code Modelling of the C-Mod Divertor”, presented at the 15th International Conference on Plasma Surface Interactions in Controlled Fusion Devices, Gifu, Japan, May, 2002.
- [3] B. Lipschultz, *et al.*, *Plasma Physics and Controlled Fusion* **44** (2002) 733.
- [4] B. LaBombard, *et al.*, “Instrumented Divertor Leakage Experiments”, Idea presented at the Alcator C-Mod Ideas Forum, December, 2001.
- [5] C. S. Pitcher, *et al.*, “Divertor bypass in the Alcator C-Mod tokamak”, *Rev. Sci. Instr.* **72** (2001) 103.

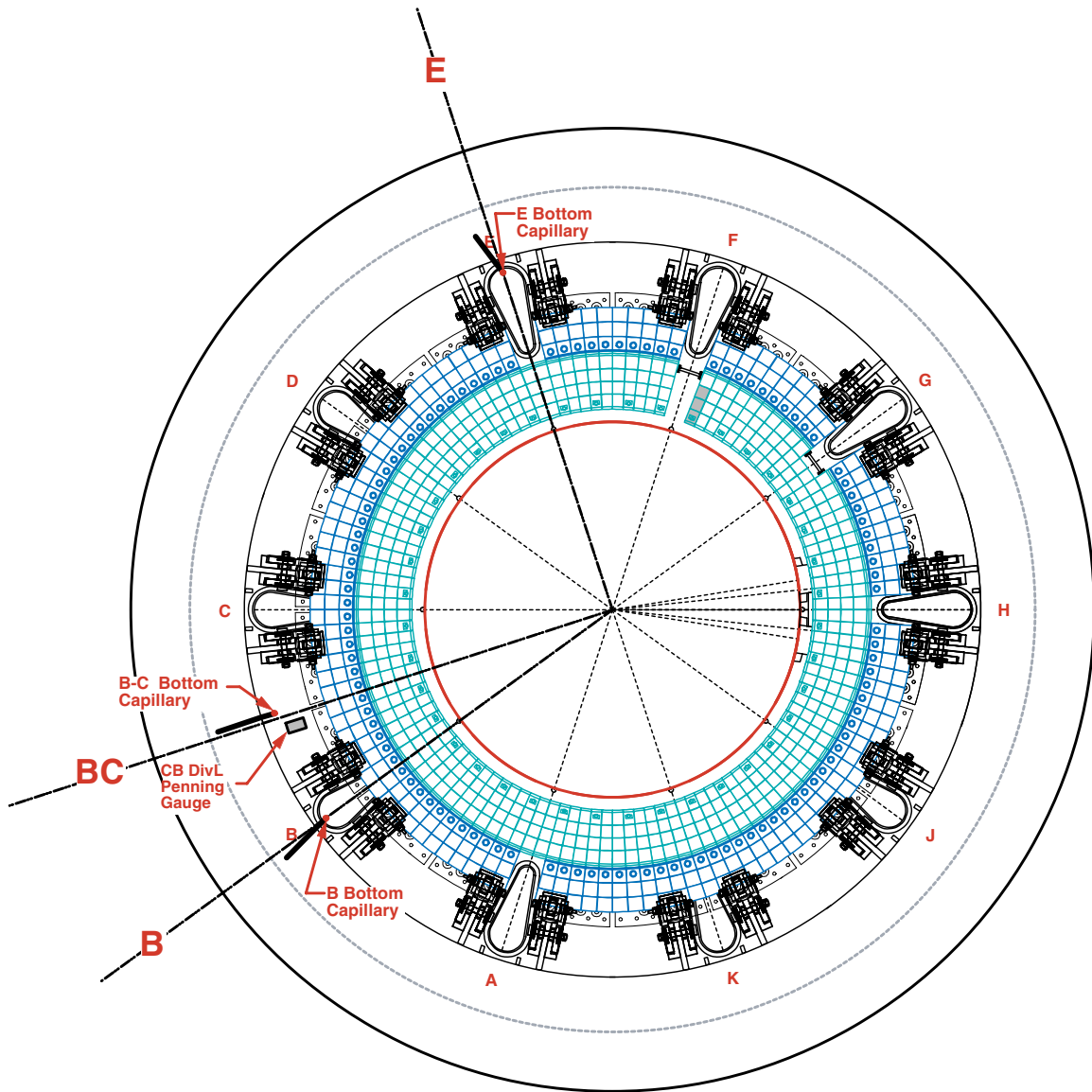


Fig. 1. Plan view of floor tiles and outer divertor mounting hardware. Locations of three gas-puff capillaries (floor level) and one in-situ Penning gauge are indicated.

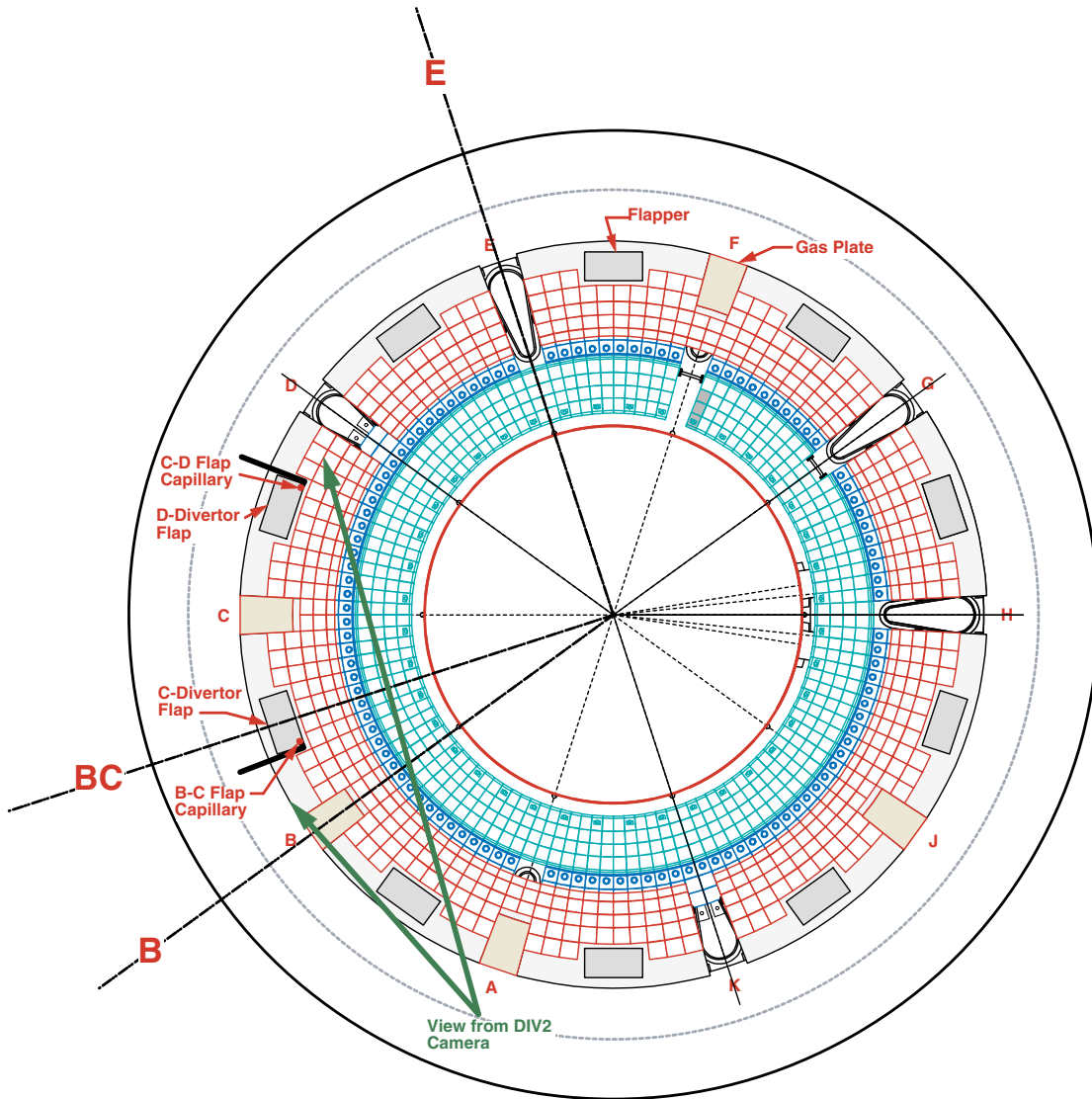


Fig. 2. Plan view of floor tiles with outer divertor tiles, gas plates, and flapper locations overlaid. D-alpha emission above two flaps is imaged from DIV2 camera. Locations of two gas-puff capillaries above flappers are indicated.

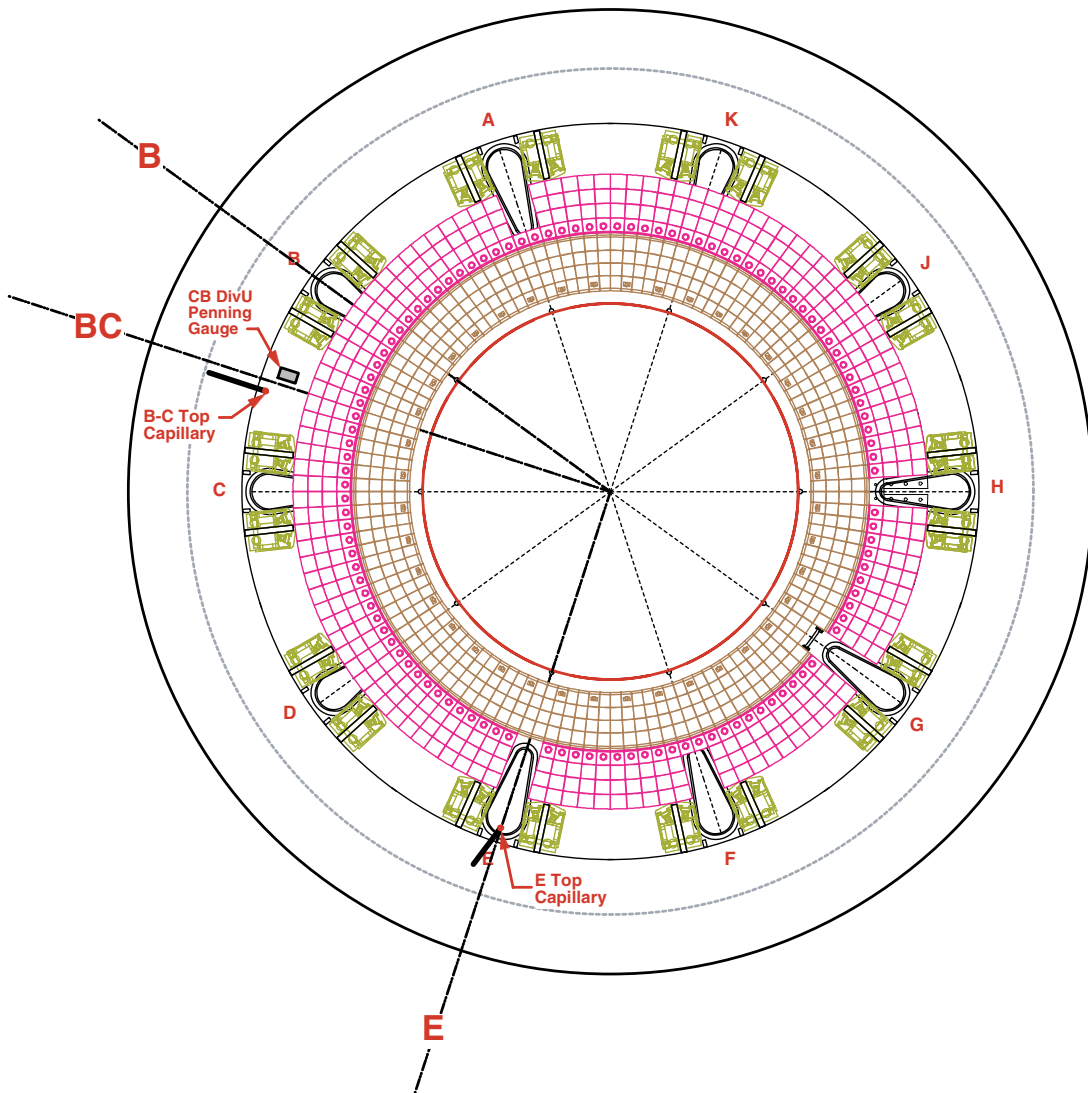


Fig. 3. View of ceiling tiles and gusset protection tiles. Locations of two gas-puff capillaries (ceiling level) and one in-situ Penning gauge (broken) are indicated.

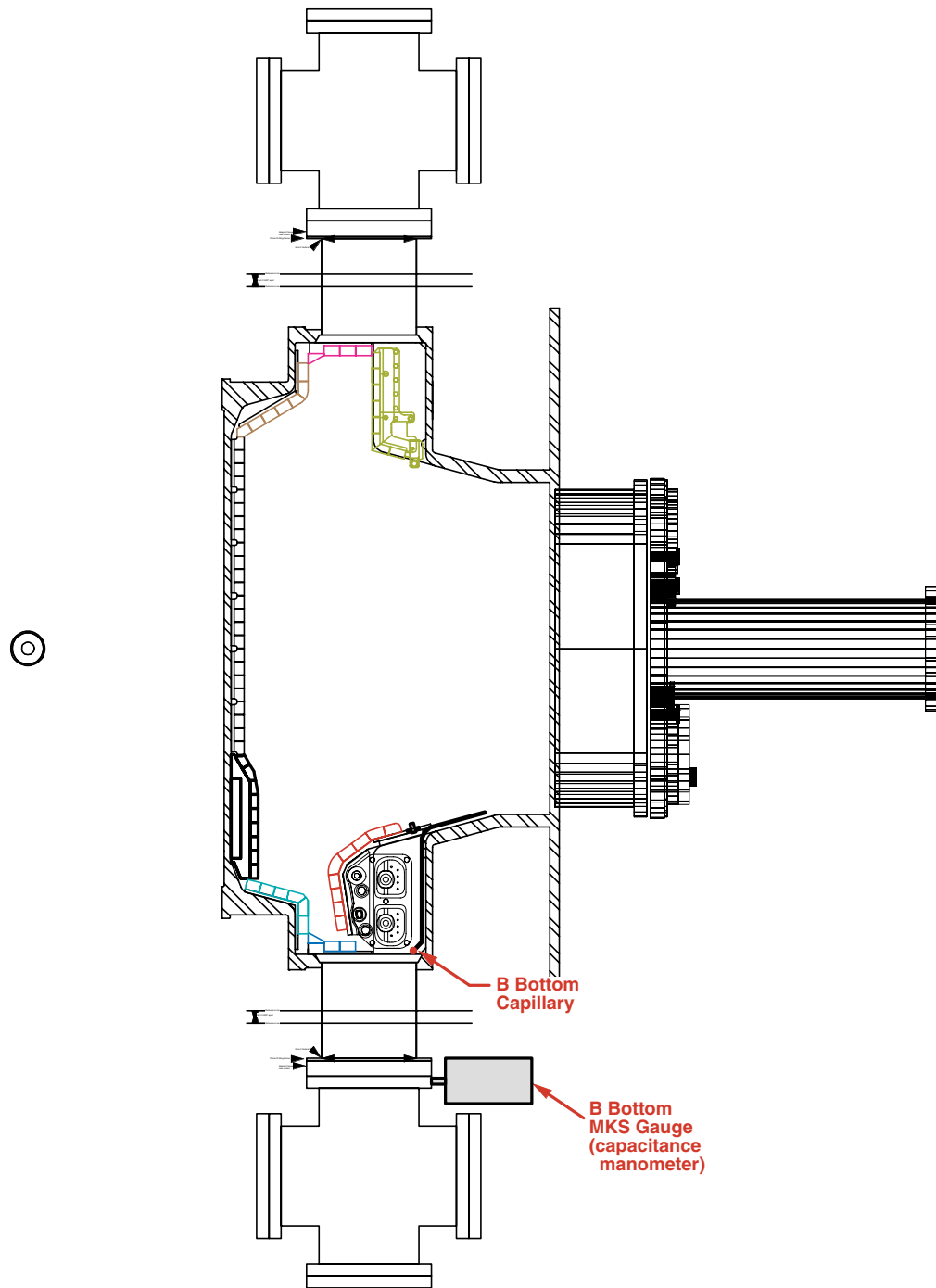


Fig. 4. Cross-section at toroidal location B ("at port"). Location of gas-puff capillary and capacitance manometer are indicated.

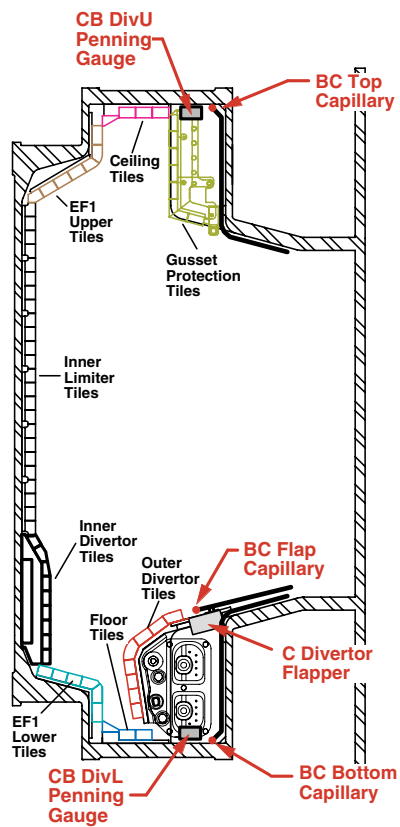


Fig. 5. Cross-section at toroidal location BC ("between ports"). Locations of three gas-puff capillaries, flapper, and two in-situ Penning gauges are indicated.

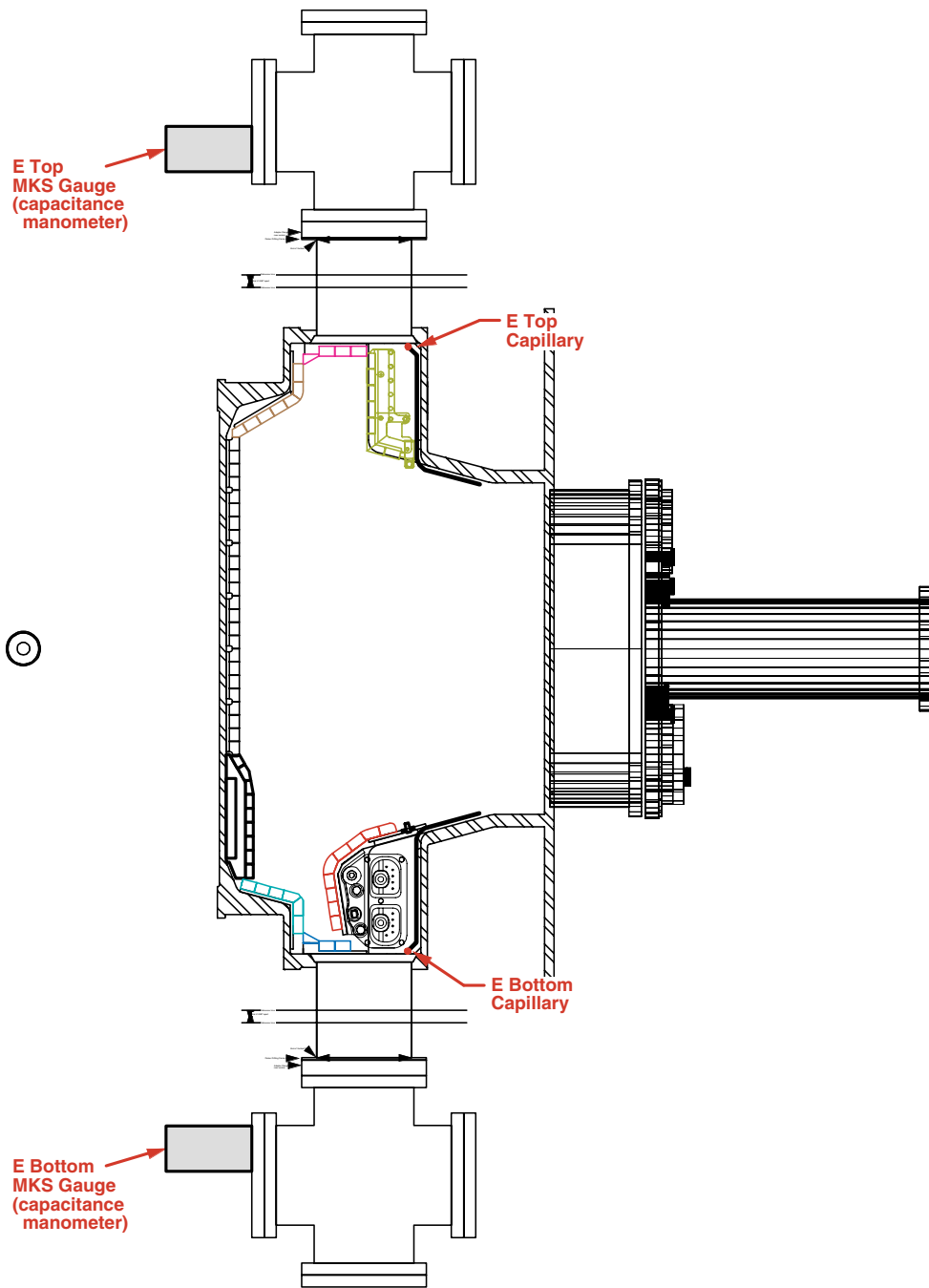


Fig. 6. Cross-section at toroidal location E ("at port"). Location of gas-puff capillaries and capacitance manometers are indicated.

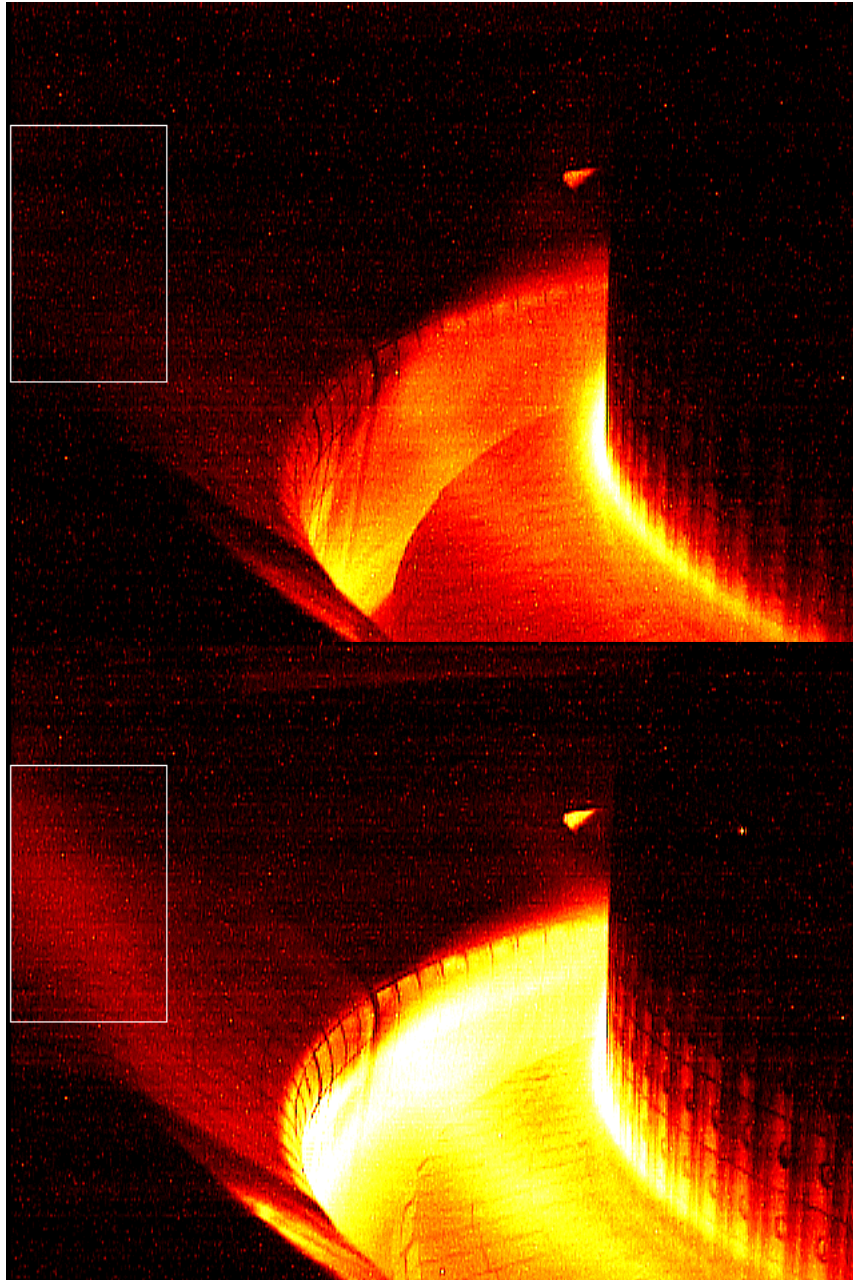


Fig. 7 - View from DIV2 camera on shot#1020725026, filtered for D_{α} light. Top frame - prior to gas puffed from BC Flap capillary. Bottom frame - during gas puff from BC Flap capillary. Note that the emission from the divertor also increases in the bottom frame as a result of the increase in core plasma density. A brightness signal versus time is formed by summing the signals from pixels within the white rectangular box.

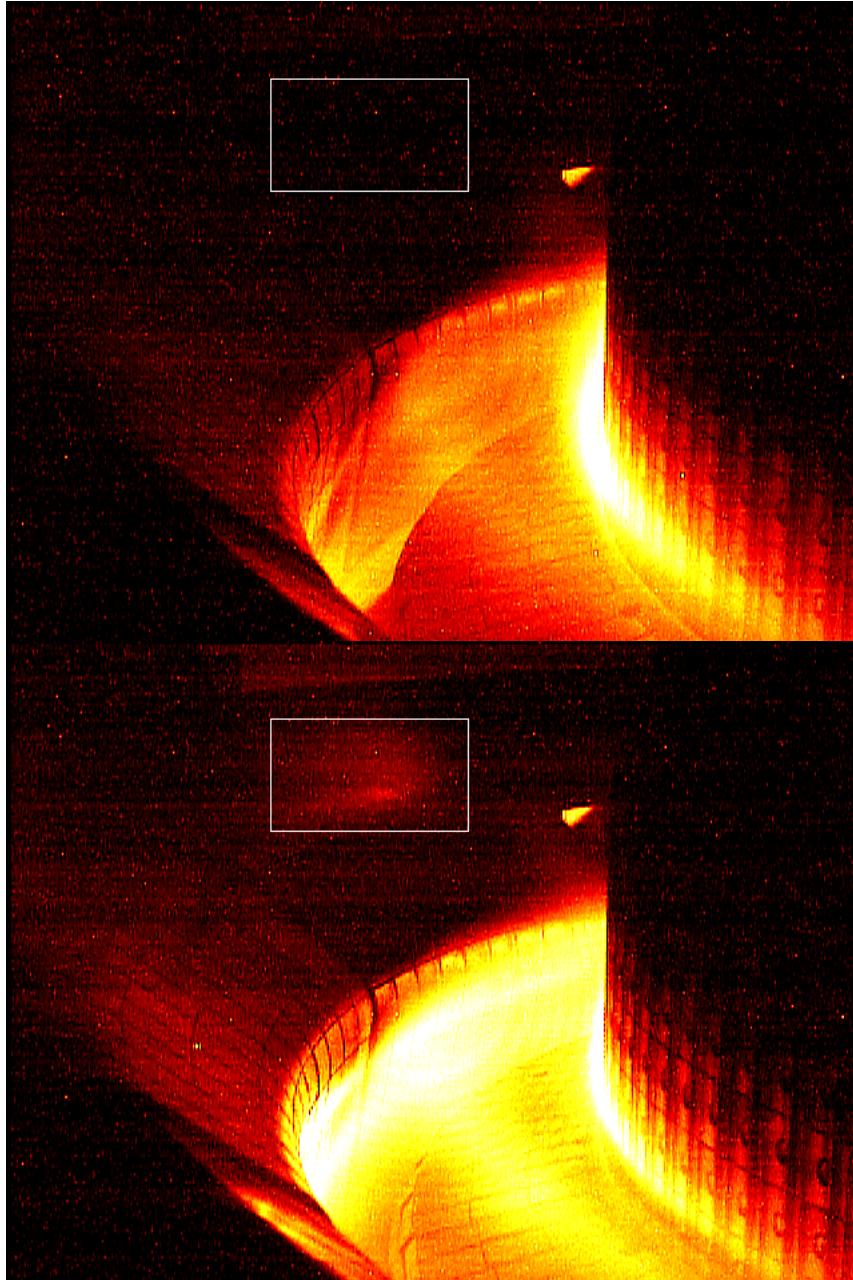


Fig. 8 - View from DIV2 camera on shot#1020725030, filtered for D α light. Top frame - prior to gas puffed from CD Flap capillary. Bottom frame - during gas puff from CD Flap capillary. Again, the emission from the divertor has increased in the bottom frame as a result of the increase in core plasma density. A brightness signal versus time is formed by summing the signals from pixels within the white rectangular box.

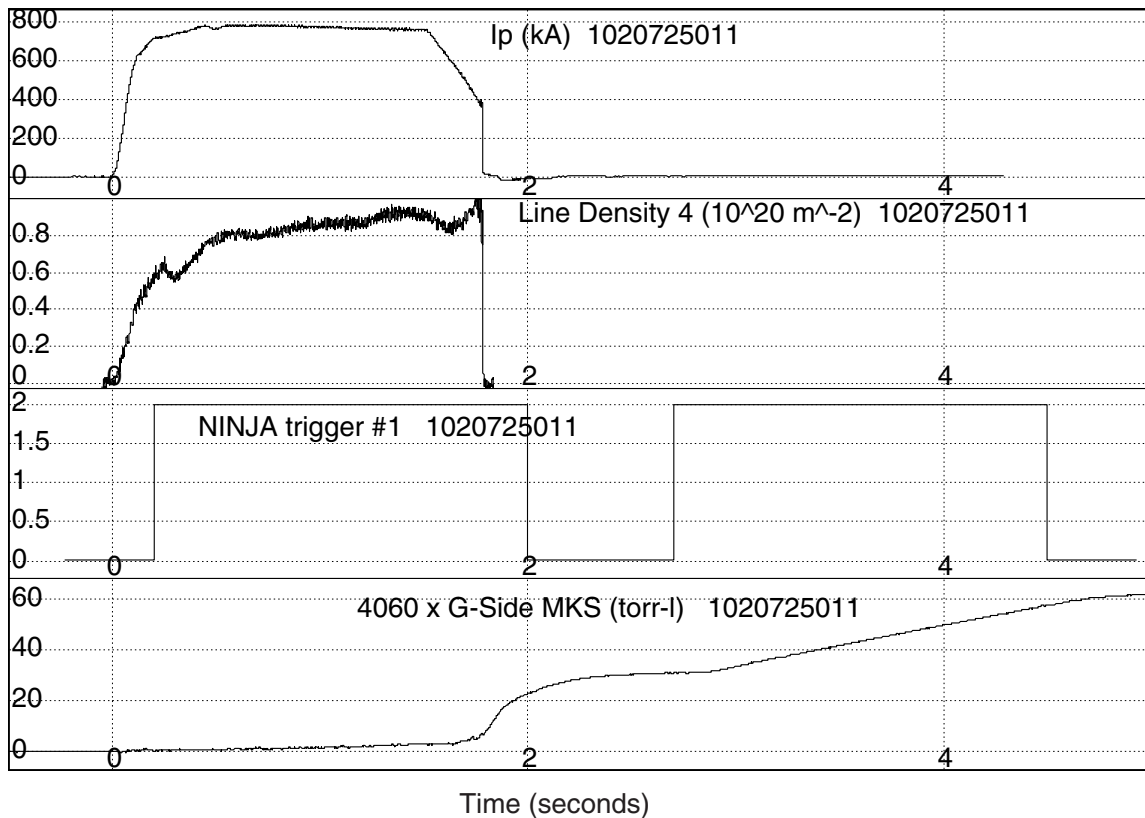


Fig. 9 - Representative discharge showing traces of plasma current, line-integral density, trigger pulse to NINJA capillary valve, and resultant molecular gas inventory in the vacuum chamber as measured by the G-Side MKS gauge. The vacuum chamber volume is 4060 liters. Therefore, the gas inventory after the discharge is 4060 times the G-Side MKS gauge pressure reading. Since the two trigger pulses are identical (and the plenum pressures are virtually unchanged), the rate of change of gas inventory observed during the second pulse is taken to be a measure of the gas throughput through the capillary during either pulse.

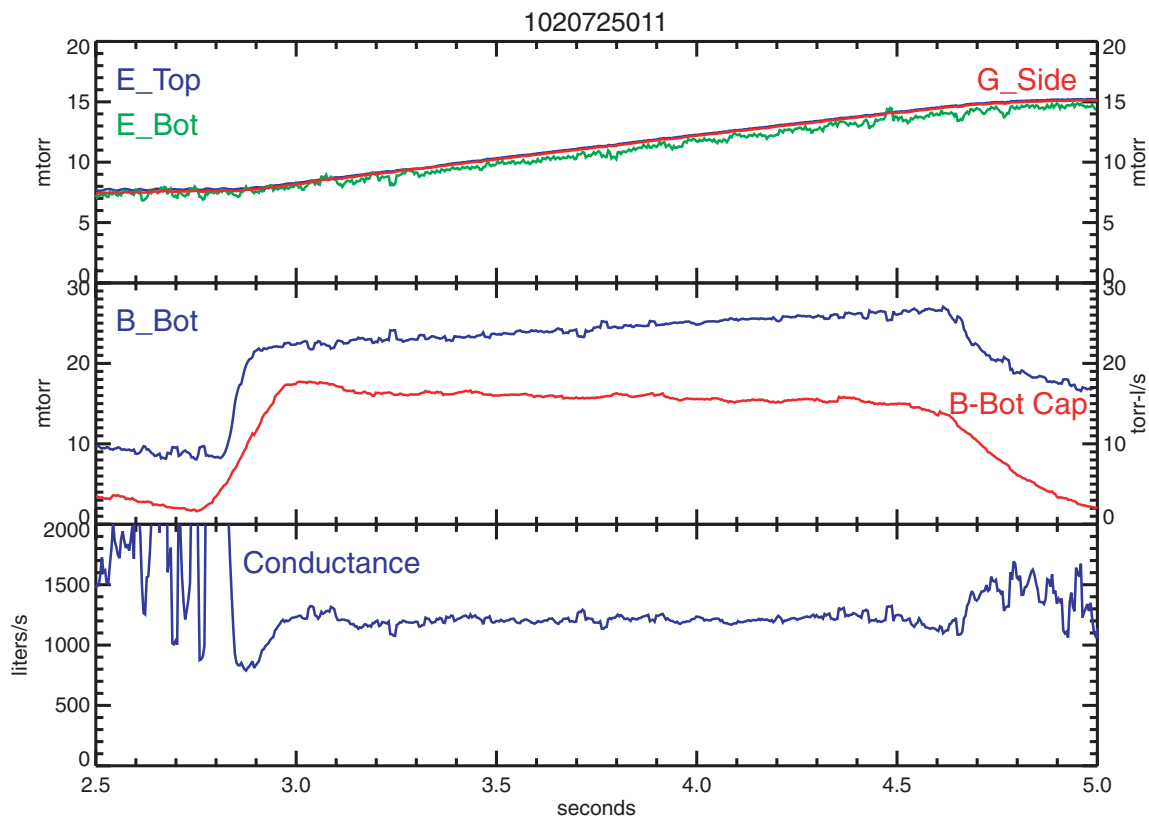


Fig. 10 - Computation of vacuum conductance away from the capillary located at B-Bottom. Top trace- three MKS gauges in the vacuum chamber show good agreement. The B-Bottom MKS gauge (B_Bot) shows a pressure jump as the B-Bottom capillary (B-Bot Cap) is turned on (flow rate computed from pressure rise in chamber, as discussed in Fig.9). The conductance signal is defined as $B_Bot\ Cap / (B_Bot - G_Side)$.

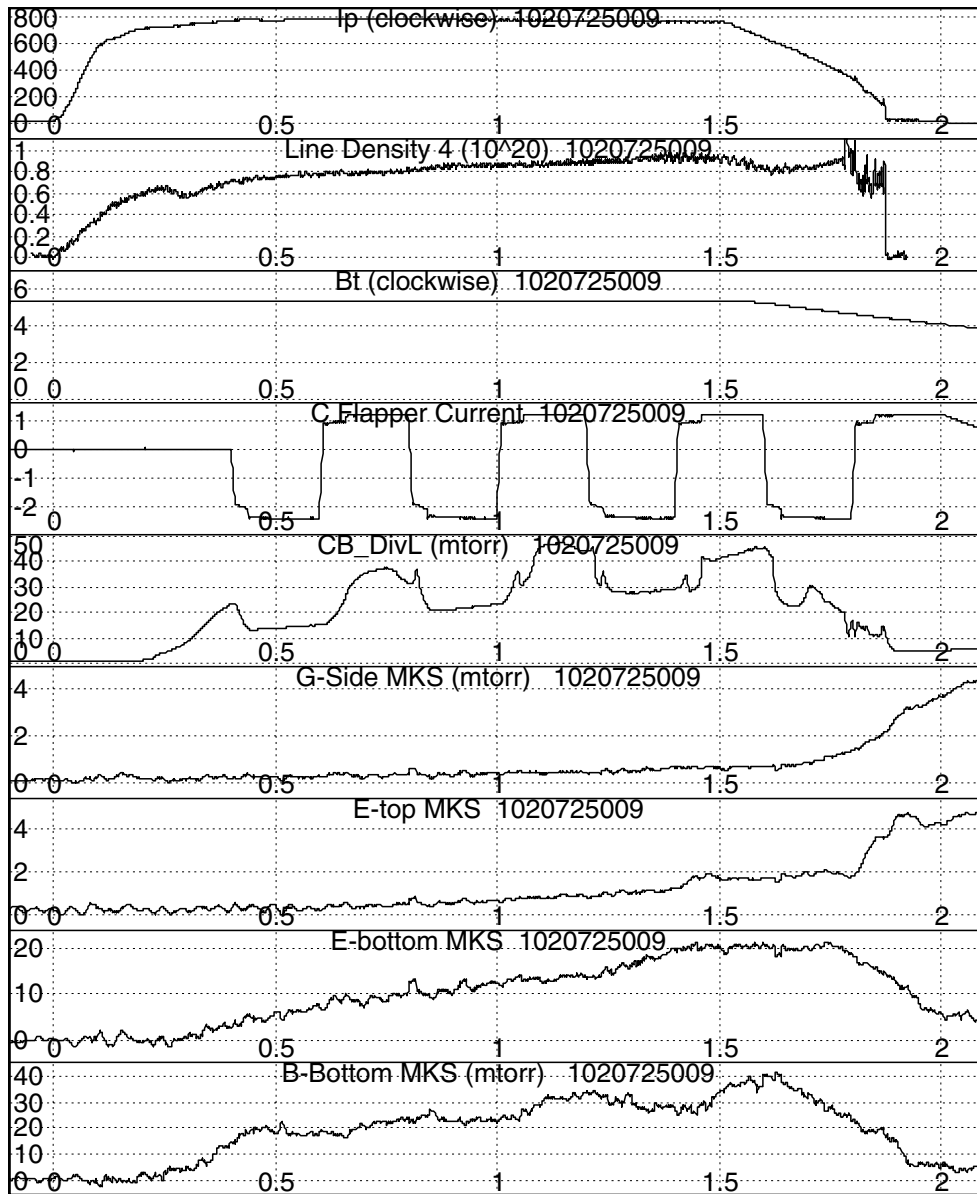


Fig. 11 - Signals from a “background” discharge (1020725009), i.e., one where gas was puffed through a capillary mounted on the A-B split limiter. This discharge is used to determine the “zero capillary flow” pressures for B-Bottom, E-Bottom and E-Top locations. The C-divertor flapper was energized to open/close 4 times. (Negative current drives a torque to open the flapper.) Note that the CB_DivL Penning gauge responds with a decreased pressure when the flap is open and an increased pressure when the flap is closed. The B-Bottom MKS gauge shows a slight modulation in response to the C-divertor flapper begin open/closed. The toroidal field trace is shown in the third panel (Bt). Sometimes the Penning gauge response is seen to change during the time when Bt ramps down - there may be some effect in this case.

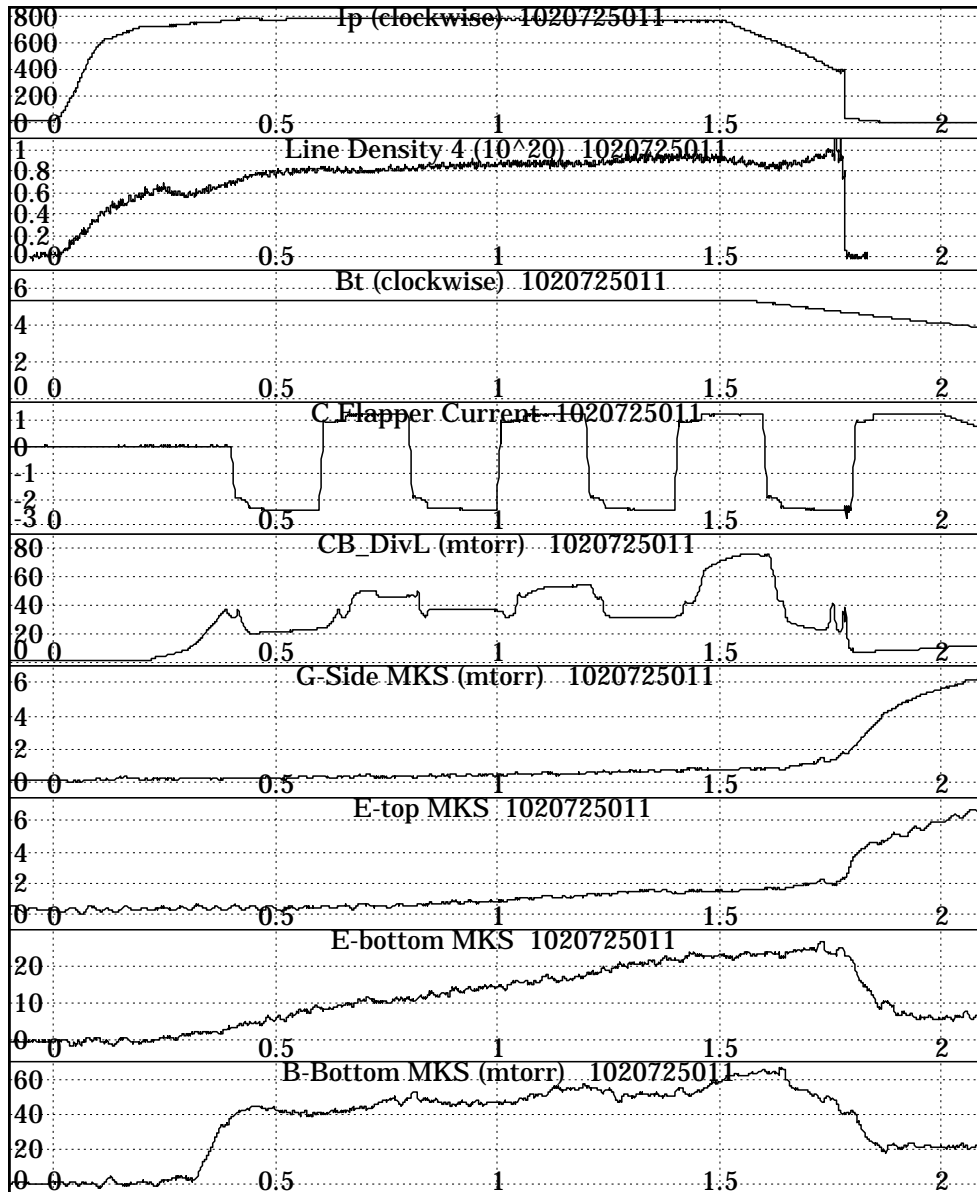


Fig. 12 - Signals from a discharge where gas was puffed through the B-Bottom capillary (shot #1020725011). The panels are the same as in Fig. 11. Note the increased pressures recorded on the B-Bottom MKS gauge.

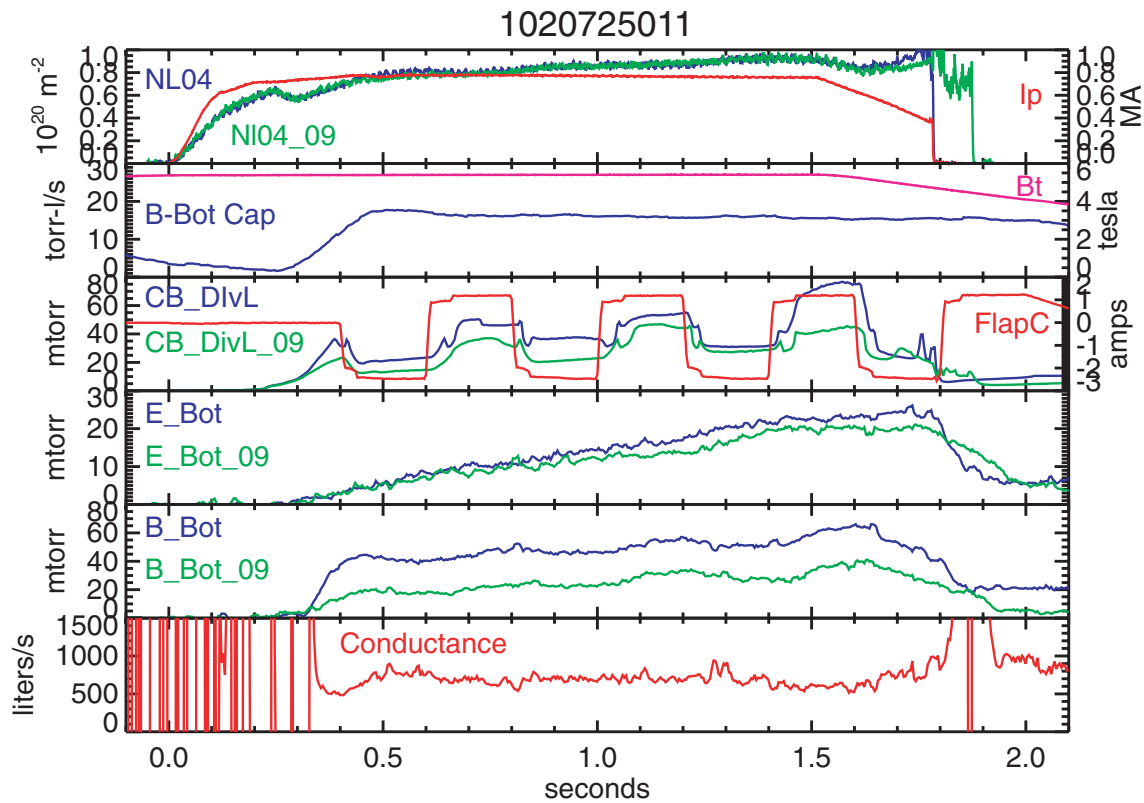


Fig. 13 - Computation of the effective conductance (i.e., conductance in the presence of plasma) away from the capillary located at B-Bottom. Signals in green are from the “background” plasma (shot #1020725009). All other signals are from shot #1020725011. The line-integral density (NL04) is essentially the same in these two shots. The consequence of the gas puffed through the B-Bottom capillary (B-Bot Cap, flow rate of ~15 torr-liters/s) is to cause the B-bottom MKS gauge pressure to rise (B_Bot) relative to the baseline discharge. The effective conductance is computed as $(B_Bot\ Cap)/(B_Bot - B_Bot_09)$, which is the flow rate divided by the change in pressure at B-Bottom. Note that the pressure under the flapper (CB_DivL) rises in response to the B-Bottom capillary puff. Also, E-Bottom MKS rises slightly, suggesting a non-negligible toroidal conductance pathway.

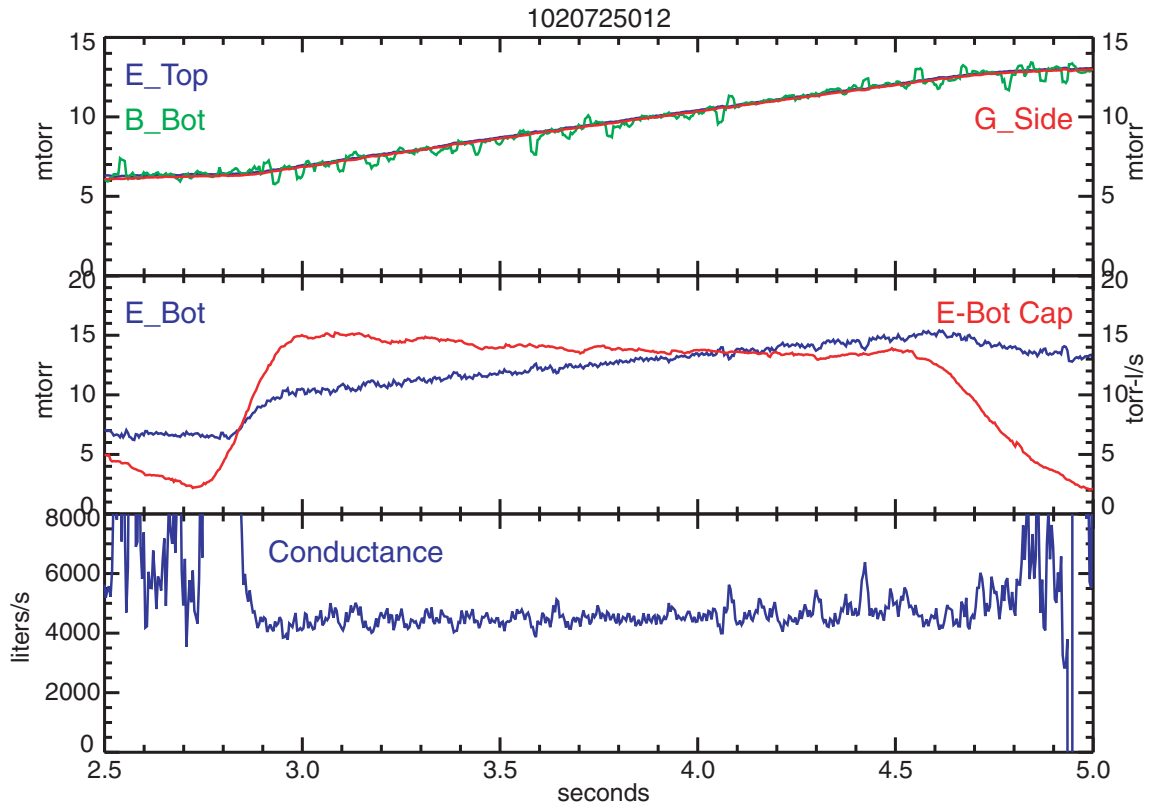


Fig. 14 - Computation of vacuum conductance away from the capillary located at E-Bottom. Analysis follows that of Fig. 10. Vacuum conductance is ~4500 liters/s.

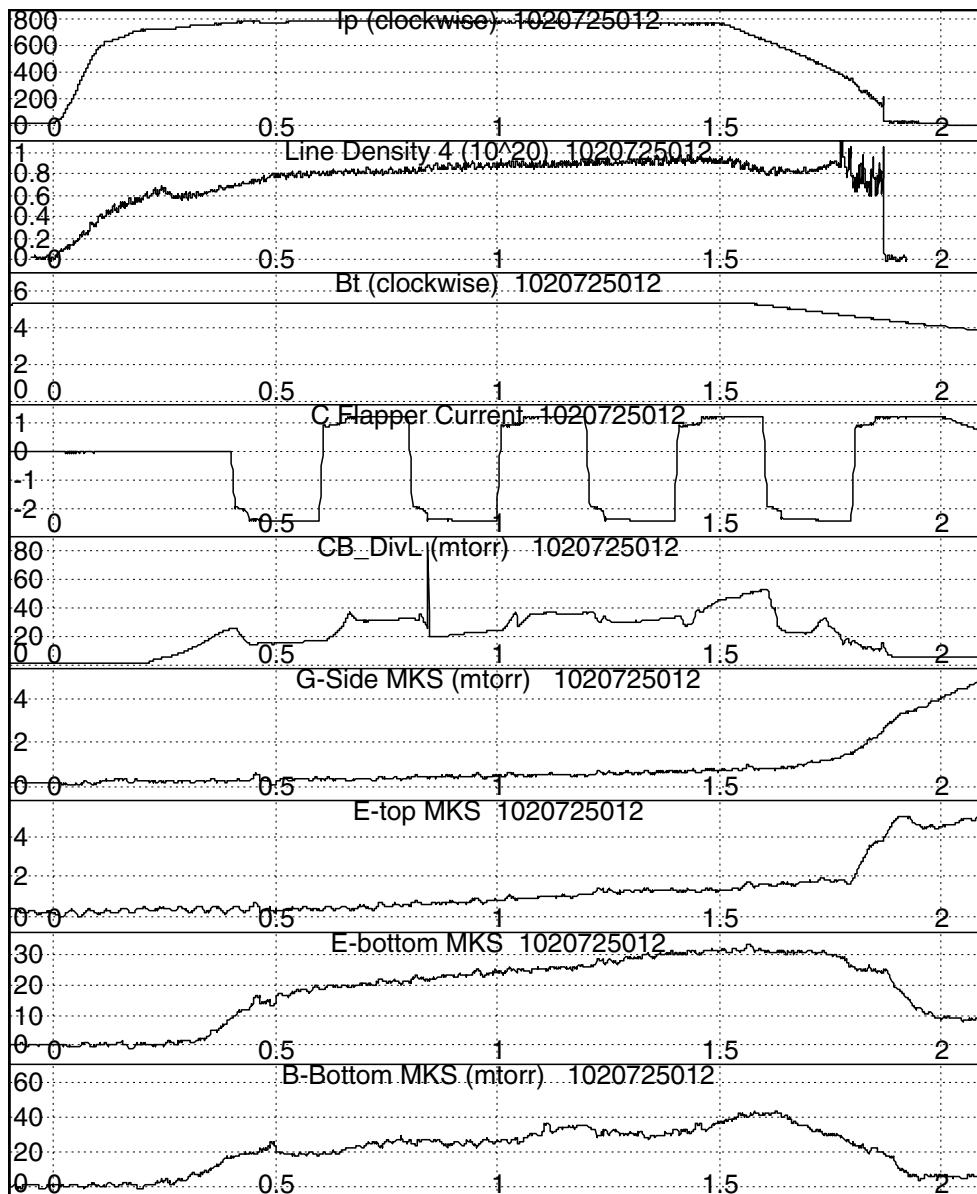


Fig. 15 - Signals from a discharge where gas was puffed through the E-Bottom capillary (shot #1020725012). The panels are the same as in Fig. 11. Note the increased pressures recorded on the E-Bottom MKS gauge relative to the “background” discharge shown in Fig. 11.

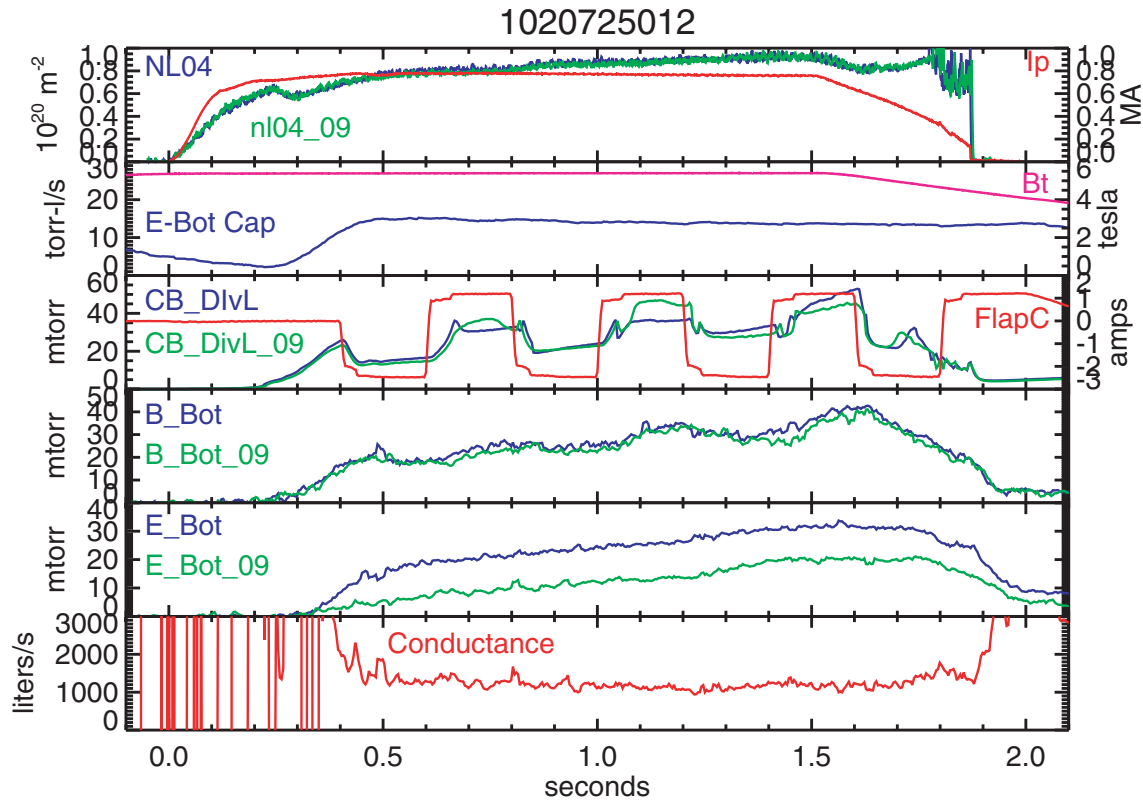


Fig. 16 - Computation of the effective conductance away from the capillary located at E-Bottom. Signals in green are from the background plasma (shot #1020725009). All other signals are from shot #1020725012. The line-integral density trace (NL04) is well matched in these two shots. The consequence of the gas puffed through the E-Bottom capillary (E-Bot Cap) is to cause the E-bottom MKS gauge pressure to rise (E_Bot) relative to the baseline discharge. The effective conductance is computed as $(E_Bot\ Cap)/(E_Bot - E_Bot_09)$, which is the flow rate divided by the change in pressure at E-Bottom. Note that the pressure under the flapper (CB_DivL) does not appear to change in response to the E-Bottom capillary puff; The variation appears to be caused by the “mode-jumping” behavior of the Penning gauge. Also, the B-Bottom MKS time traces are essentially identical; Even the modulation caused by the C-divertor flap (FlapC) opening/closing is reproduced.

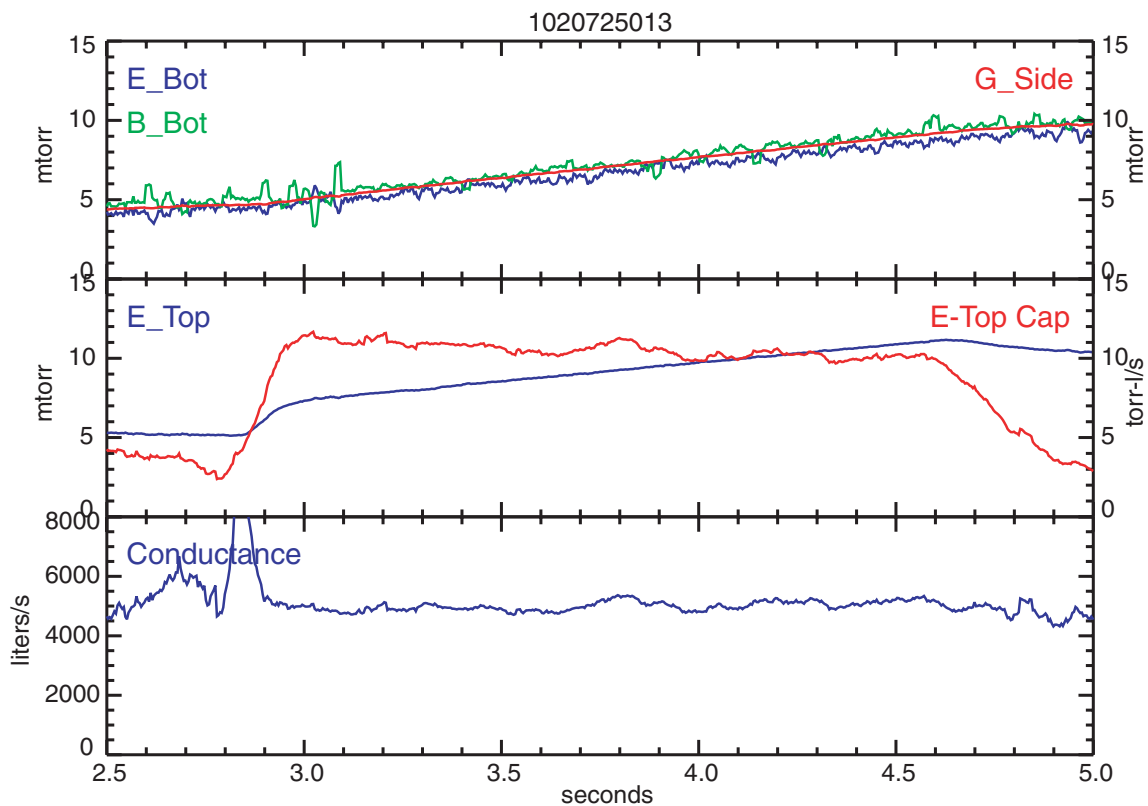


Fig. 17 - Computation of vacuum conductance away from the capillary located at E-Top. Analysis follows that of Fig. 10. Vacuum conductance is ~5000 liters/s.

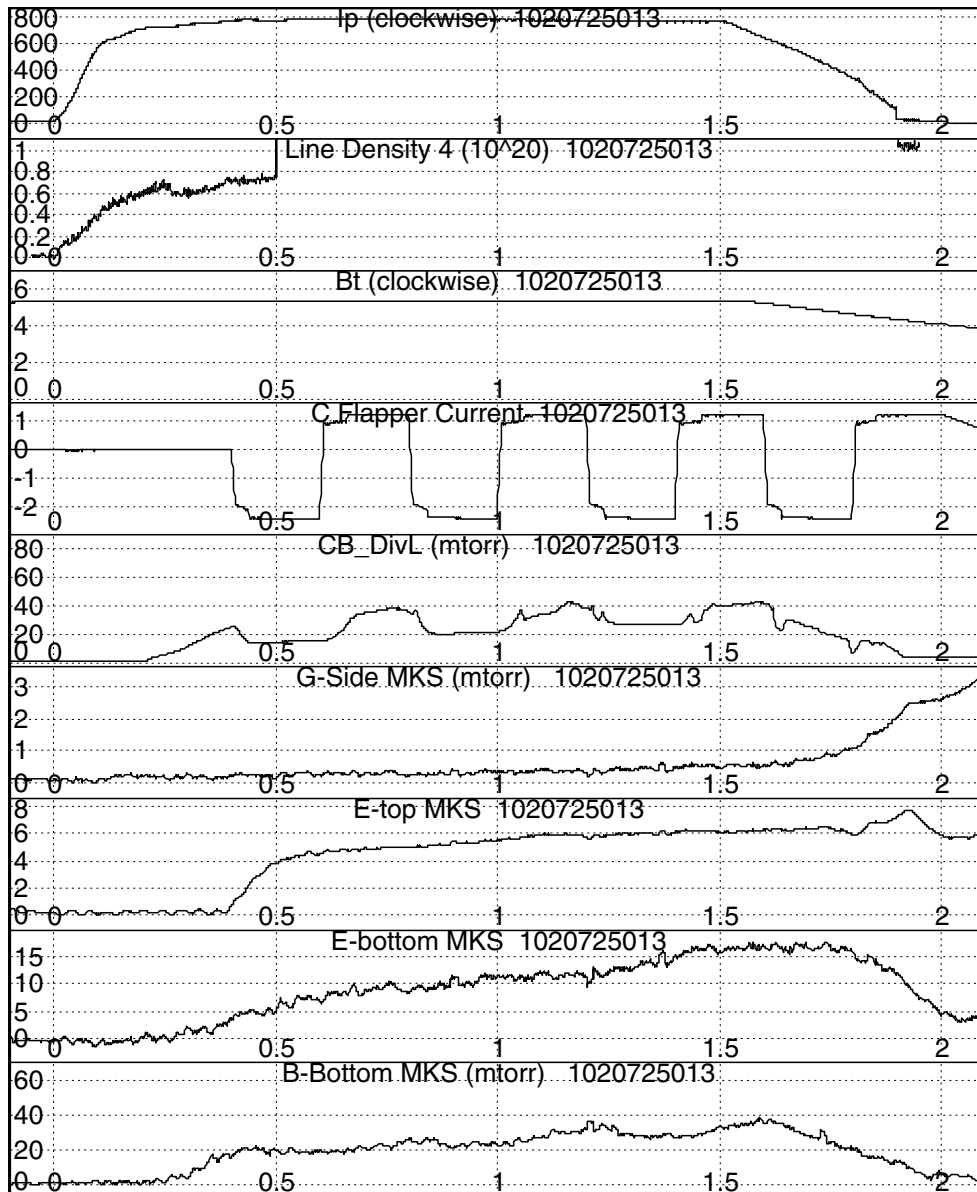


Fig. 18 - Signals from a lower single null (SNL) discharge where gas was puffed through the E-Top capillary (shot #1020725013). The panels are the same as in Fig. 11. Note the increased pressures recorded on the E-top MKS gauge relative to the “background” discharge shown in Fig. 11. The interferometer had a problem on this shot, leading to only a partial data trace in the second panel.

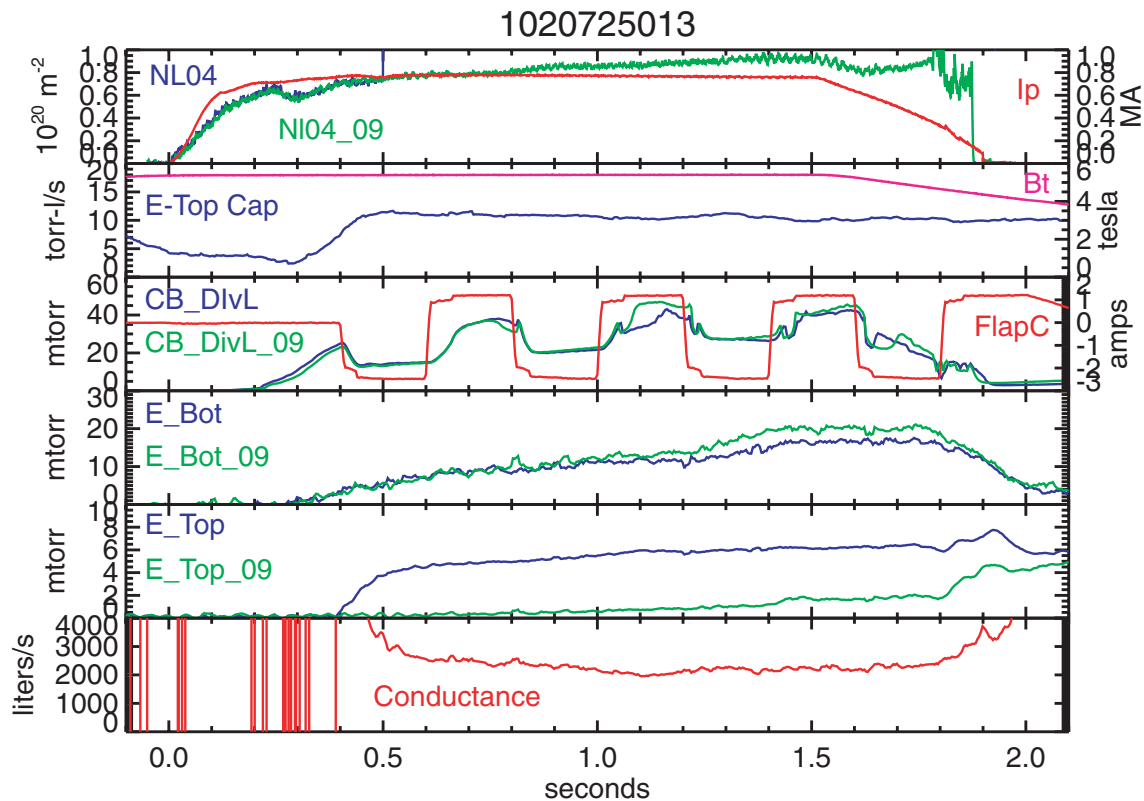


Fig. 19 - Computation of the effective conductance away from the capillary located at E-Top during a lower single null discharge (SNL). Signals in green are from the background plasma (shot #1020725009). All other signals are from shot #1020725013. The line-integral density trace (NL04) is matched over the limited time where data is available. The consequence of the gas puffed through the E-Top capillary (E-Top Cap) is to cause the E-Top MKS gauge pressure to rise (E_Top) relative to the baseline discharge. The effective conductance is computed as $(E_Top\ Cap)/(E_Top - E_Top_09)$, which is the flow rate divided by the change in pressure at E-Top. Note again that the pressure under the flapper (CB_DivL) does not appear to change in response to the E-Top capillary puff; the variation relative to the background discharge appears to be caused by the “mode-jumping” behavior of the Penning gauge. The E-Bottom MKS time traces do no overlap after 1.2 seconds. Nevertheless, the computed conductance remains essentially unchanged during this time, indicating that the lack of a perfect match is not so important.

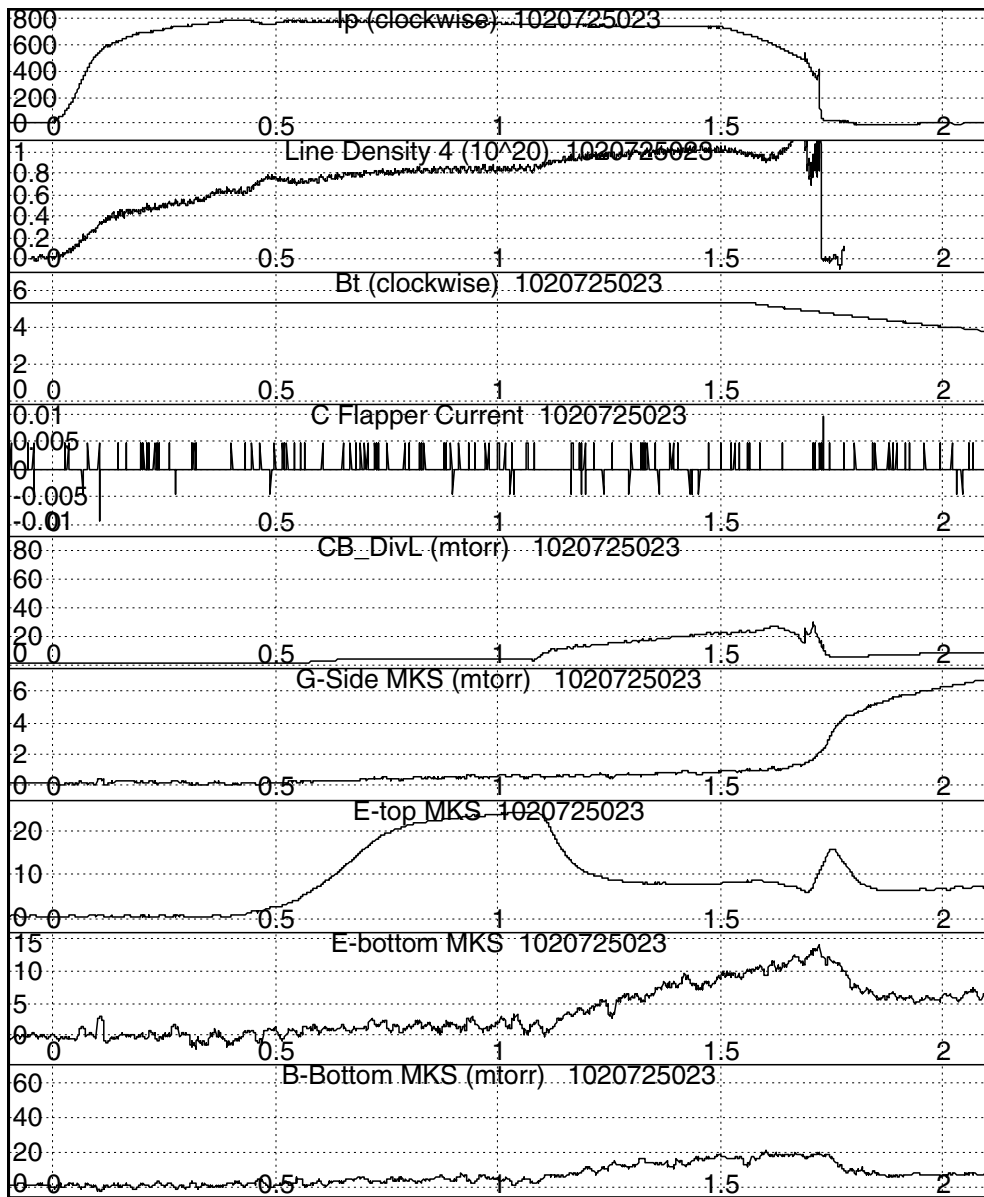


Fig. 20 - Signals from an upper single null (SNU) “background” discharge (1020725023), i.e., one where gas was puffed through a capillary mounted on the A-B split limiter. This discharge is used to determine the “zero capillary flow” pressure for the E-Top location. The C-divertor flapper was not operated. There is a divertor-detachment/MARFE event after 1.1 seconds that causes the E-Top pressure to drop and the pressures in the lower divertor to rise.

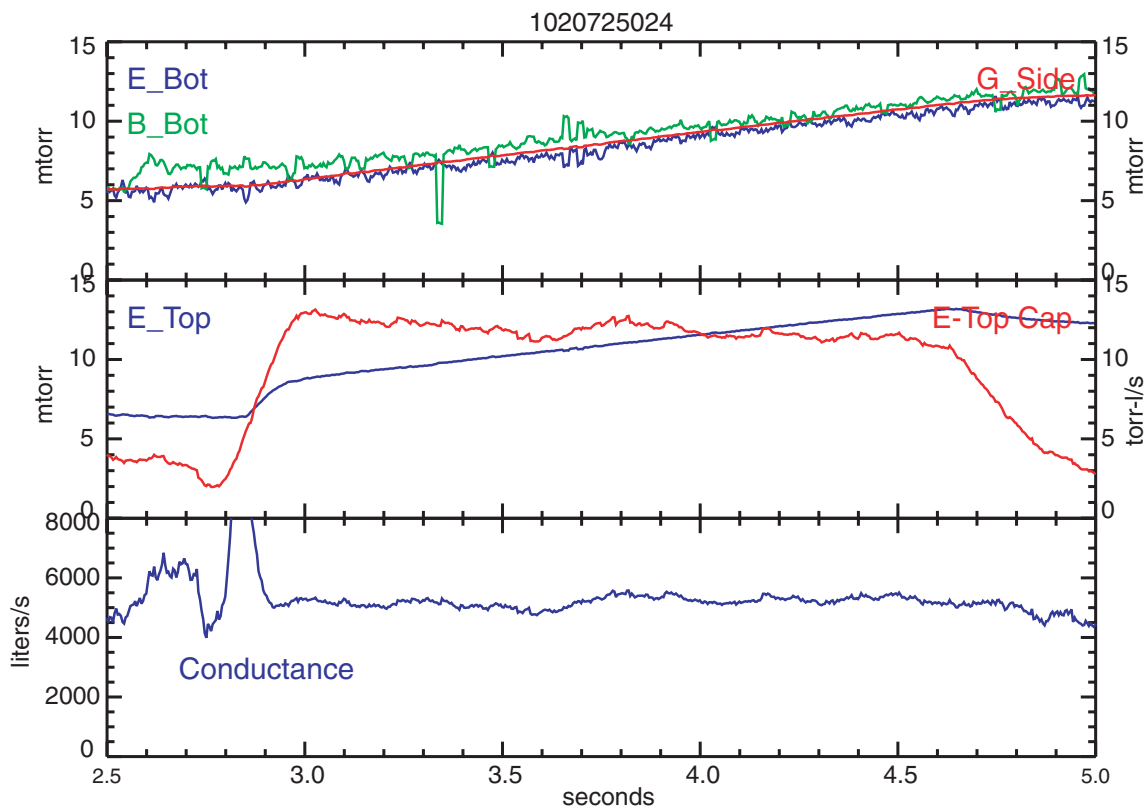


Fig. 21 - Another separate computation of vacuum conductance away from the capillary located at E-Top. Analysis is identical to that of Fig. 17. Vacuum conductance is ~5200 liters/s, within about 5% of that computed in Fig. 17.

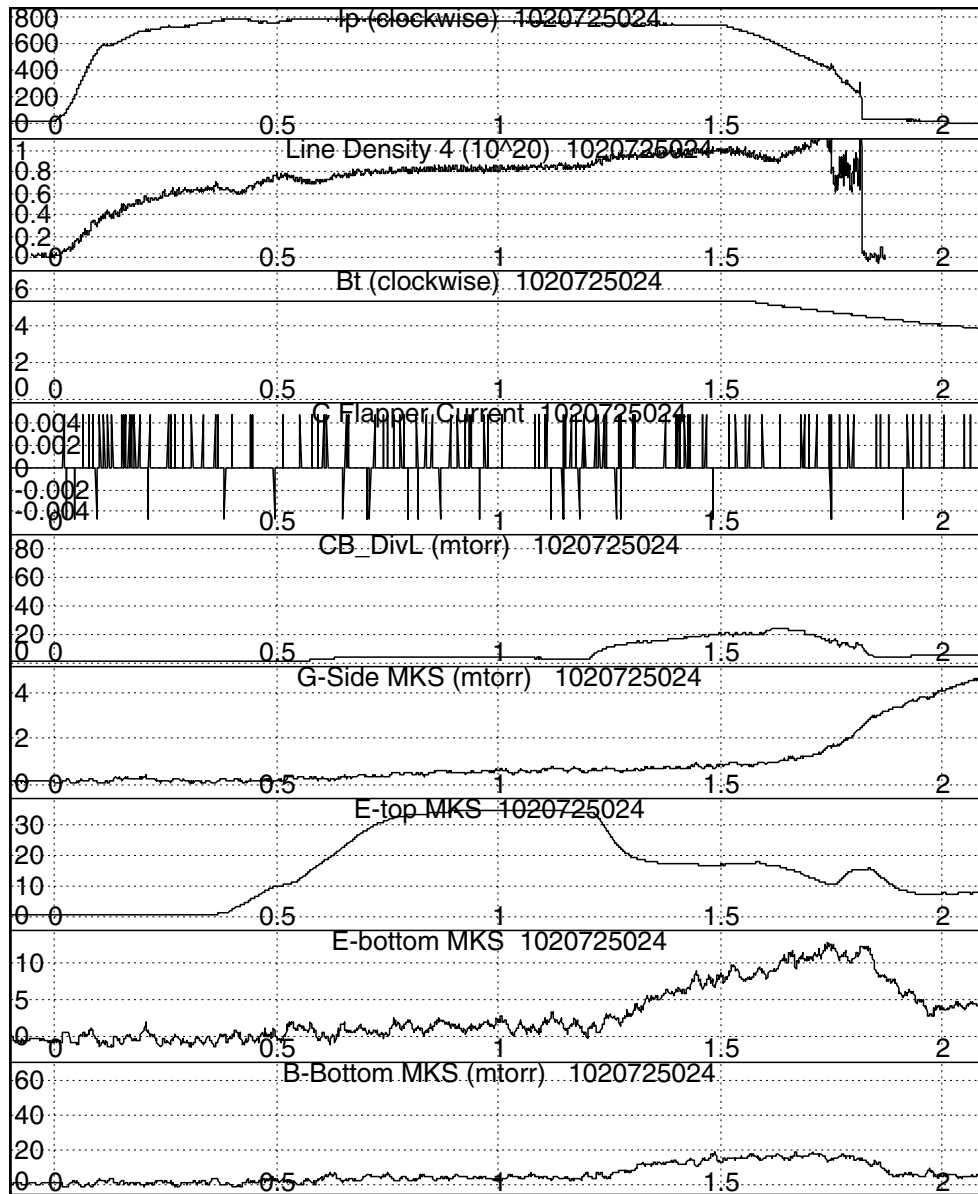


Fig. 22 - Signals from an upper single null (SNU) discharge where gas was puffed through the E-Top capillary (shot #1020725024). The panels are the same as in Fig. 20. Another divertor-detachment/MARFE event occurs after 1.2 seconds that causes the E-Top pressure to drop and the pressures in the lower divertor to rise. The pressures recorded on the E-top MKS gauge are increased relative to the background discharge shown in Fig. 20.

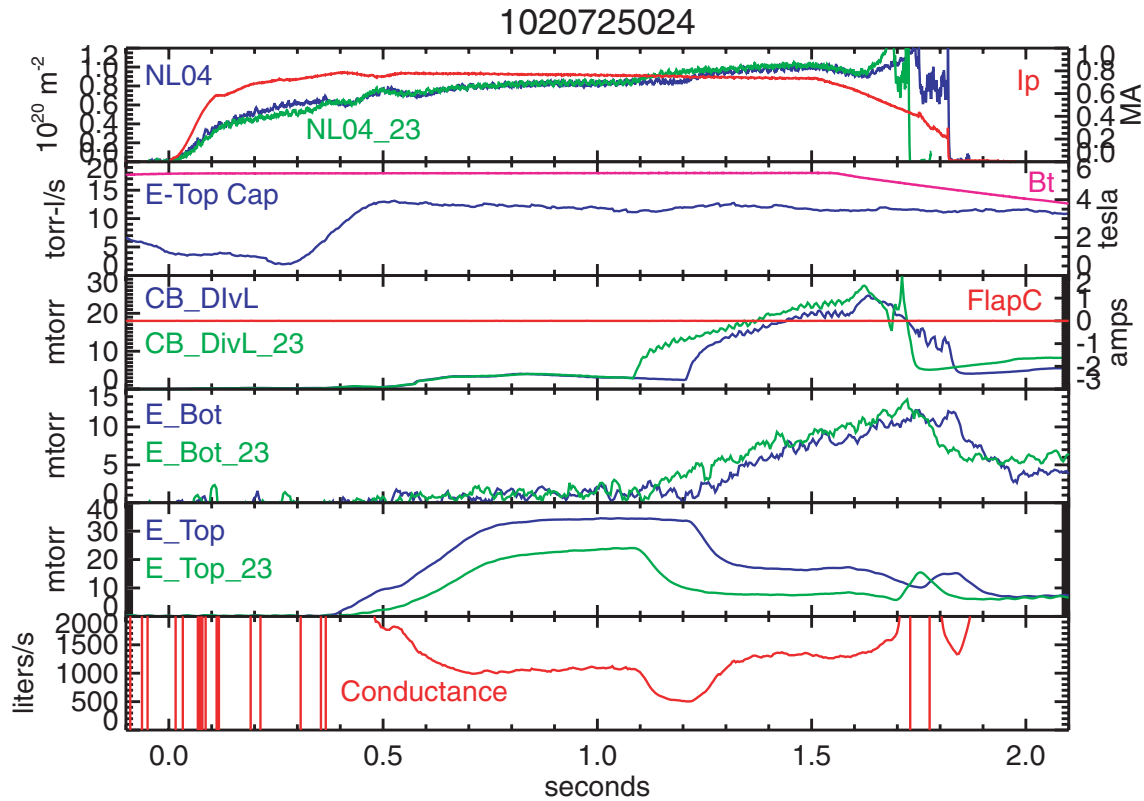


Fig. 23 - Computation of the effective conductance away from the capillary located at E-Top during an upper single null discharge (SNU). Signals in green are from the “background” plasma (shot #1020725023). All other signals are from shot #1020725024. The line-integral density trace (NL04) is well matched except during the different time when the detachment/MARFE phenomenon occurs. Prior to detachment/MARFE time, the discharges are well matched. The consequence of the gas puffed through the E-Top capillary (E-Top Cap) is to cause the E-Top MKS gauge pressure to rise (E_Top) relative to the baseline discharge. The effective conductance is computed as $(E_Top\ Cap)/(E_Top - E_Top_23)$, which is the flow rate divided by the change in pressure at E-Top.

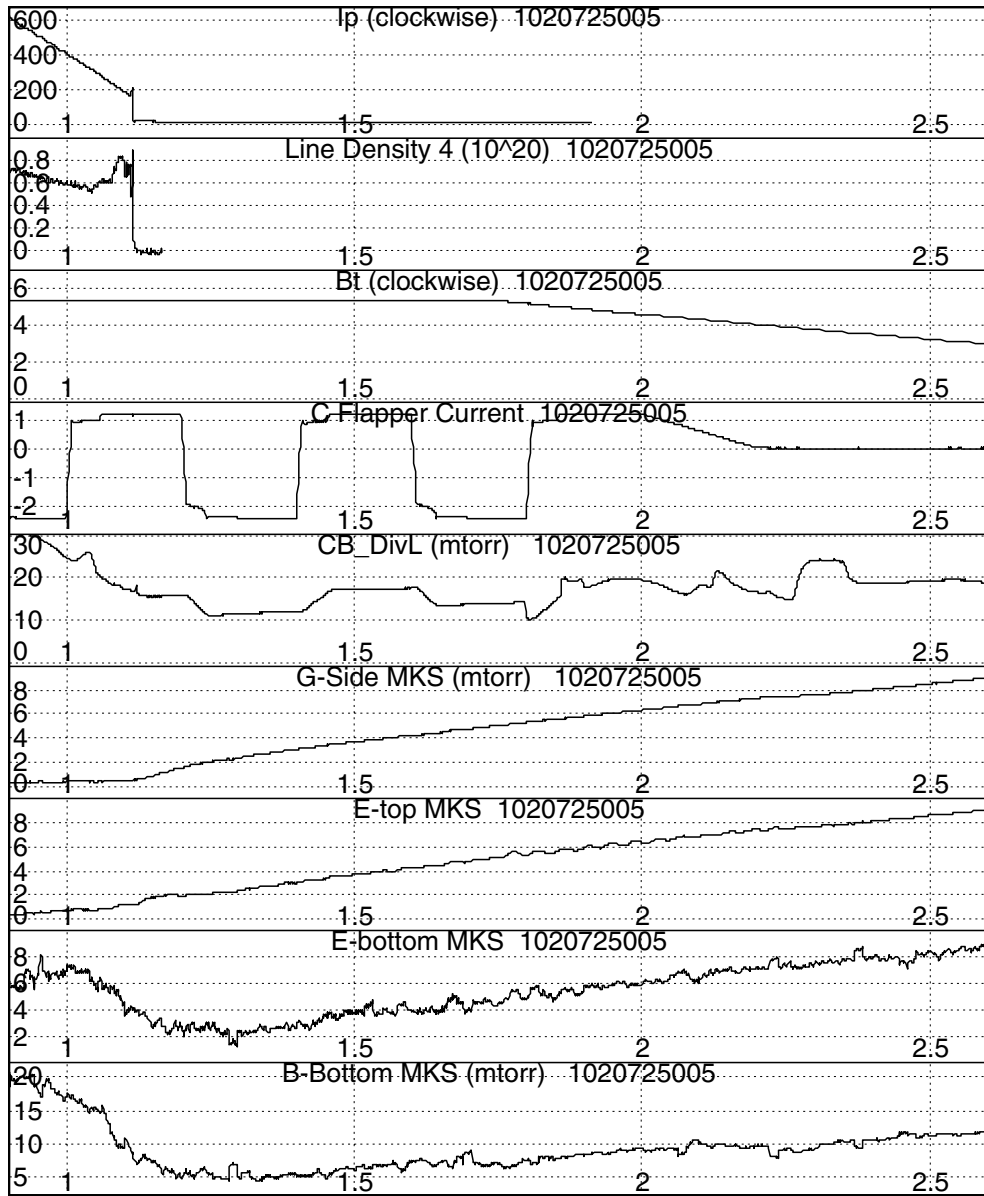


Fig. 24 - Signals just after a discharge (shot #1020725005) while gas is puffed through the BC-Bottom capillary. The panels are the same as in previous figures. The toroidal magnetic field is maintained constant well after the discharge (to 1.75 seconds) so that the CB_DivL Penning gauge continues to operate. From 1.12 to 1.8 seconds the C-divertor flap starts closed, opens, closes and opens again. In response, the pressure recorded by the CB_DivL gauge modulates cleanly during this time.

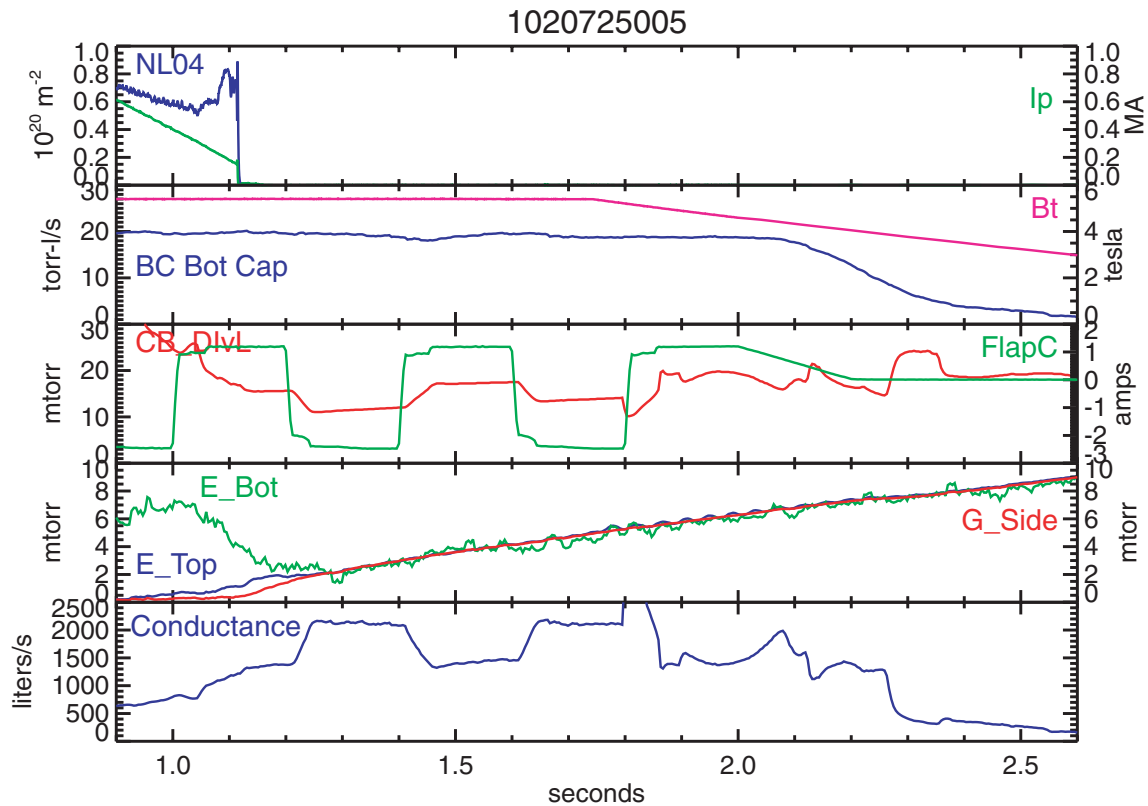


Fig. 25 - Computation of the vacuum conductance away from the capillary located at BC-Bottom with C-divertor flap open and closed. In response to gas puffed through the BC-Bottom capillary (BC Bot Cap), the pressure under the C-divertor module (CB_DivL) increases above that in the rest of the torus (as seen by three MKS gauge signals in fourth panel). The time of interest is between 1.12 seconds (after plasma termination) and before 1.8 seconds (when Penning gauge exhibits a “mode-change” behavior). During this time, the pressure under the C-divertor module is cleanly modulated by the C-divertor flap (FlapC) opening and closing. The vacuum conductance is computed as $(BC\ Bot\ Cap)/(CB_DivL - G_Side)$, which is the flow rate divided by the difference in pressure between under the C-divertor and the rest of the vacuum chamber.

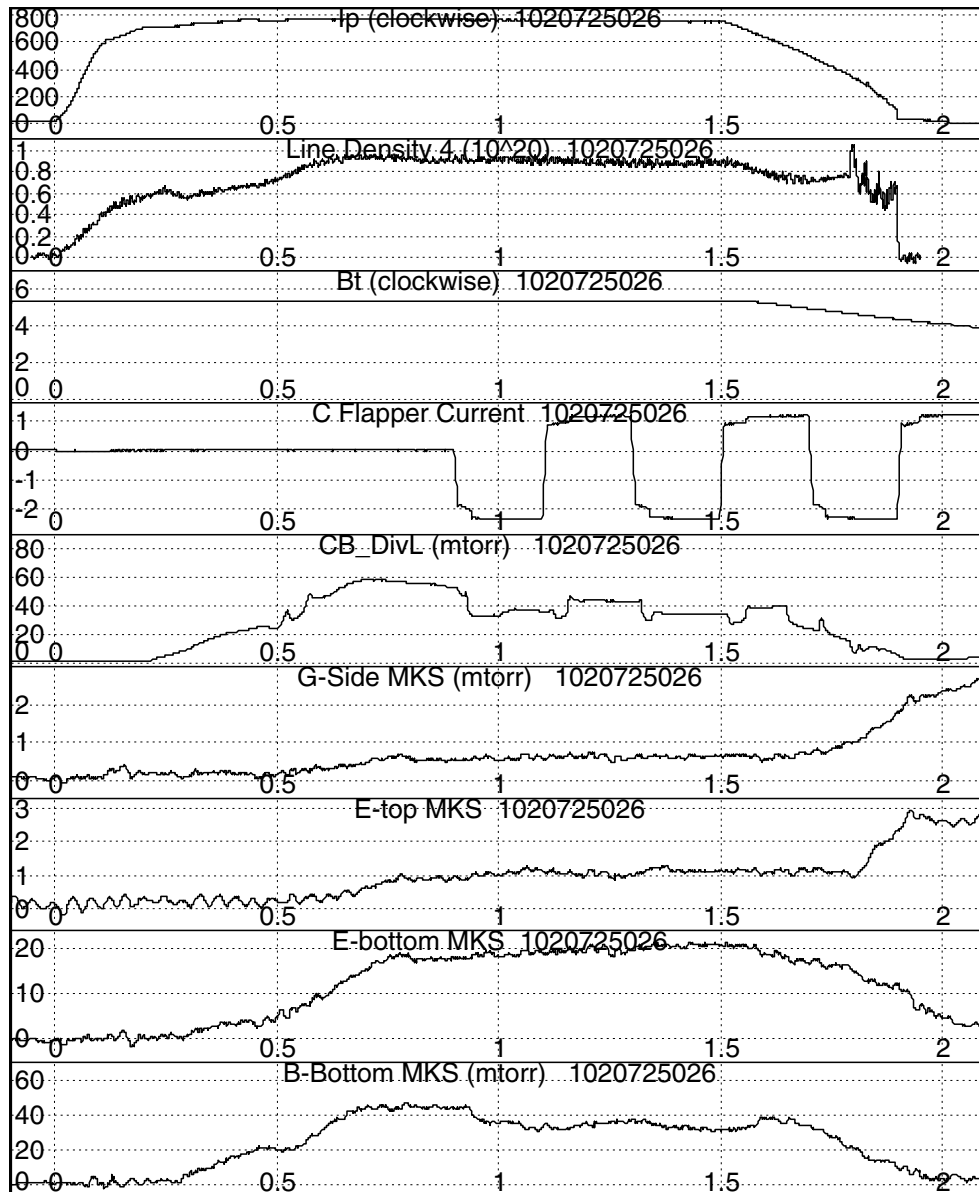


Fig. 26 - Signals from a discharge (shot #1020725026) where a strong, short-duration gas puff was programmed through the B-C flap capillary (gas flow begins at about 0.5 seconds with a duration of 0.15 seconds). The C-divertor flap is programmed to subsequently open/close three cycles.

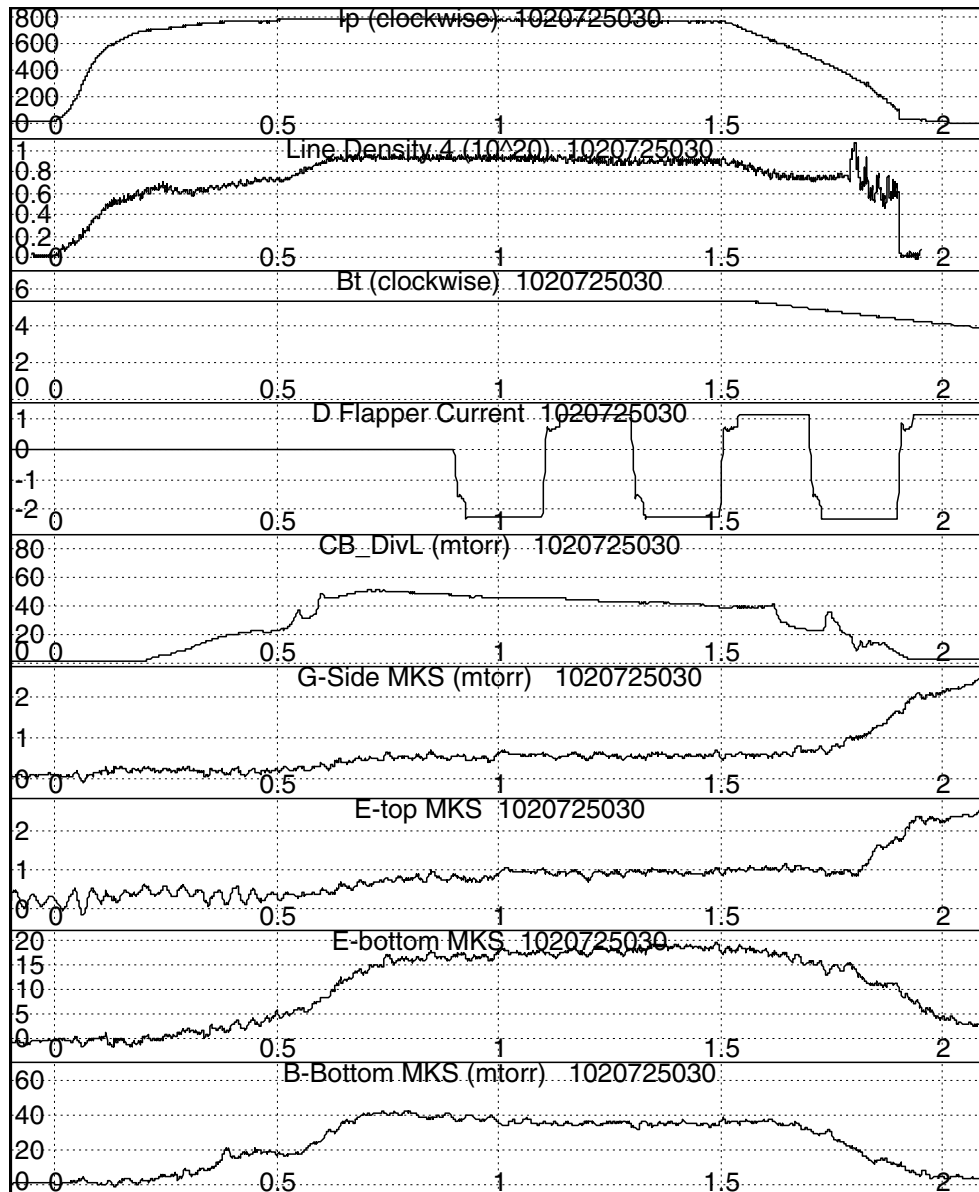


Fig. 27 - Signals from a discharge (shot #1020725030) where a strong, short-duration gas puff was programmed through the C-D flap capillary (gas flow begins at about 0.5 seconds with a duration of 0.15 seconds). The D-divertor flap is programmed to subsequently open/close three cycles.

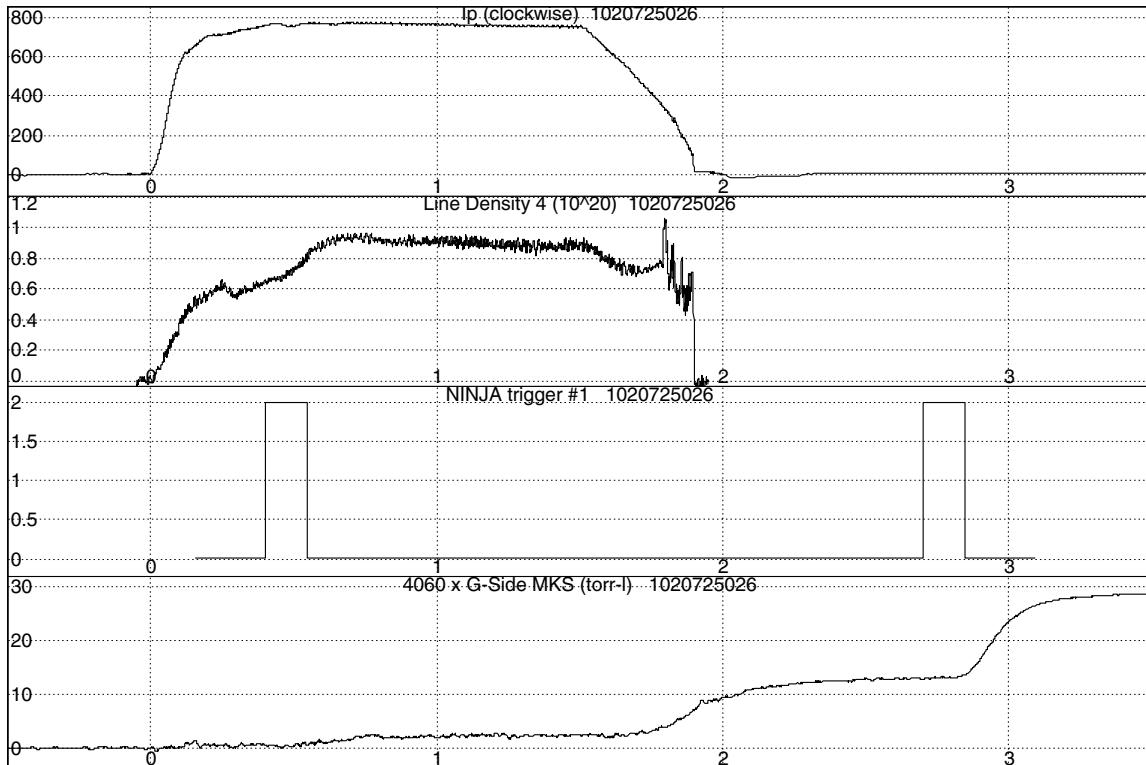


Fig. 28 - Signals from shot #1020725030 where a strong, short-duration gas puff was programmed through the C-B flap capillary (valve trigger signal shown in third panel). The flow rate during the first puff is computed from the rate of change in gas inventory (last panel) caused by an identical second puff (with trigger starting at 2.7 seconds).

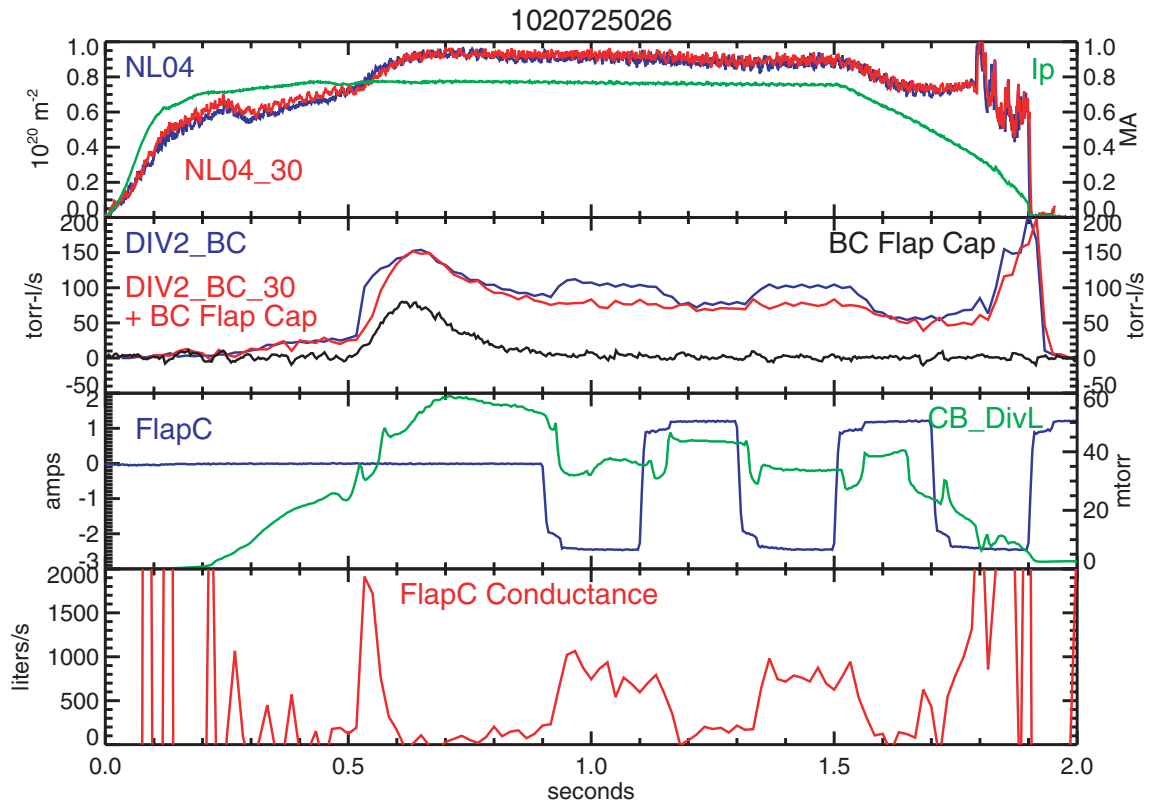


Fig. 29 - Computation of gas flow rate and effective gas conductance through C-divertor flap. The time trace of line-integral density from the “background” shot #1020725030 (NL04_30) closely matches that from shot #1020725026 (NL04). Signals “DIV2_BC” and “DIV2_BC_30” are gas-flow rates derived from the level of D_{α} light seen by the DIV2 camera in a region just above the C-divertor flap (see view in Fig. 7). “BC Flap Cap” is the gas flow rate through the B-C Flap capillary. The calibration factor between D_{α} light signal and gas flow rate is adjusted until the sum of DIV2_BC_30 plus BC Flap Cap (red trace in second panel) overlays with the DIV2_BC signal during the time when the C-divertor flap is closed. (Negative current levels on FlapC in third panel indicate torque in the direction to open the flap.) When the C-divertor flap is opened, a step increase in D_{α} light is seen, corresponding to step increase of 25 torr-liters/s in gas flow rate. In response to the flap opening, the pressure under the flap (CB_DivL) decreases. The effective conductance through the C-divertor flap (last panel) is computed from $(DIV2_BC - DIV2_BC_30 - BC\ Flap\ Cap)/(CB_DivL - G_Side_MKS)$, which is the gas flow rate through the flap divided by an estimate of the pressure difference across the flap.

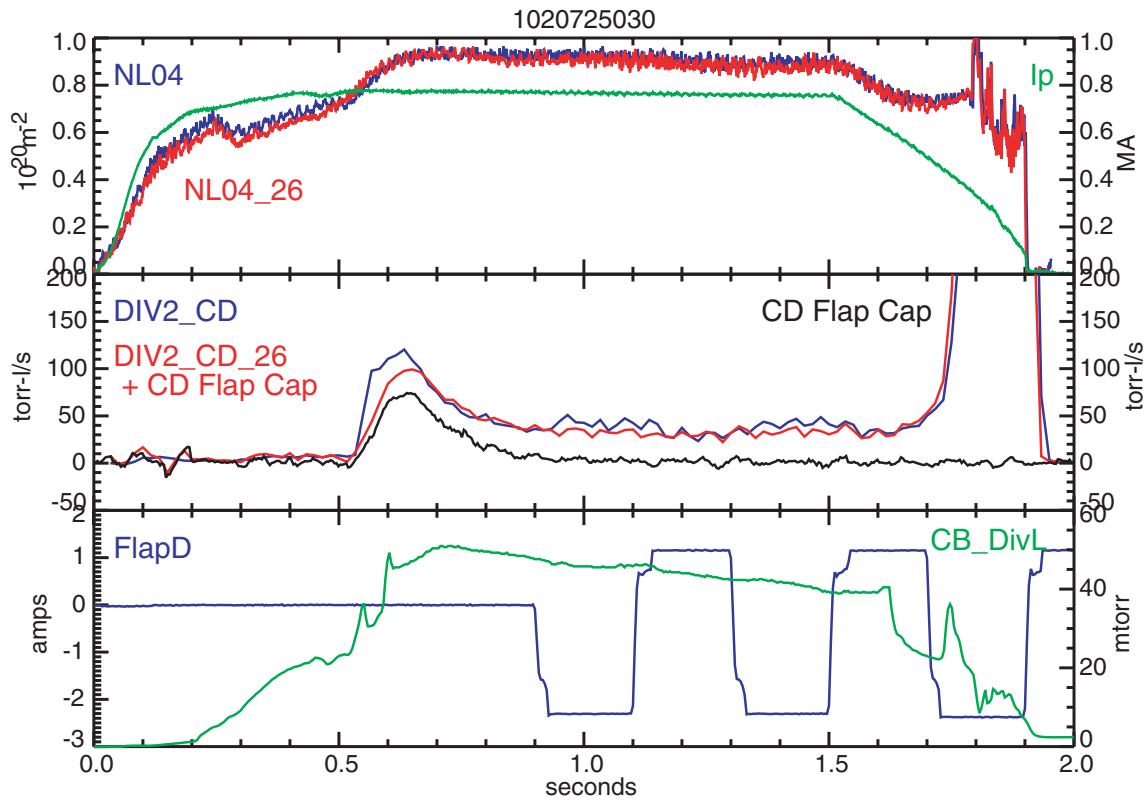


Fig. 30 - Computation of gas flow rate through D-divertor flap. The time trace of line-integral density from the “background” shot #1020725026 (NL04_26) closely matches that from shot #1020725030 (NL04). Signals “DIV2_CD” and “DIV2_CD_26” are gas-flow rates derived from the level of D_{α} light seen by the DIV2 camera in a region just above the D-divertor flap (see view in Fig. 8). “CD Flap Cap” is the gas flow rate through the C-D Flap capillary. The calibration factor between D_{α} light signal and gas flow rate is adjusted until the sum of DIV2_CD_26 plus CD Flap Cap (red trace in second panel) overlays with the DIV2_CD signal during the time when the D-divertor flap is closed. (Negative current levels on FlapD in third panel indicate torque in the direction to open the flap.) When the D-divertor flap is opened, a small step increase in D_{α} light is seen, corresponding to step increase of 10 torr-liters/s in gas flow rate. This flow rate is a factor of 2 below that deduced from the C-divertor flap which may be indicative that the pressure under the D-divertor flap is lower. As can be seen in Fig.2, the D-divertor sector is close to the “open port” at D-port.